Science of the Total Environment 502 (2015) 362–374

Contents lists available at ScienceDirect

Science of the Total Environment

journal homepage: www.elsevier.com/locate/scitotenv

The use of Pb, Sr, and Hg isotopes in Great Lakes precipitation as a tool for pollution source attribution

Laura S. Sherman [a,*], Joel D. Blum [a], J. Timothy Dvonch [b], Lynne E. Gratz [c], Matthew S. Landis [d]

[a] University of Michigan, Department of Earth and Environmental Sciences, 1100 N. University Ave., Ann Arbor, MI 48109, USA
[b] University of Michigan, Air Quality Laboratory, 1415 Washington Heights, Ann Arbor, MI 48109, USA
[c] University of Washington-Bothell, 18115 Campus Way NE, Bothell, WA 98011, USA
[d] U.S. EPA, Office of Research and Development, Research Triangle Park, NC 27709, USA

HIGHLIGHTS

- We measured Pb, Sr, and Hg isotopes in precipitation from the Great Lakes region.
- Pb isotopes suggest that deposition was impacted by coal combustion and metal production.
- Sr isotope ratios vary regionally, likely due to soil dust and coal fly ash.
- Hg isotopes vary due to fractionation occurring within facilities and the atmosphere.
- Isotope results support conclusions of previous trace element receptor modeling.

ARTICLE INFO

Article history:
Received 5 June 2014
Received in revised form 9 September 2014
Accepted 11 September 2014
Available online xxxx

Editor: Mae Sexauer Gustin

Keywords:
Heavy metals
Stable isotopes
Source attribution
Multivariate statistical receptor modeling
Wet deposition

ABSTRACT

The anthropogenic emission and subsequent deposition of heavy metals including mercury (Hg) and lead (Pb) present human health and environmental concerns. Although it is known that local and regional sources of these metals contribute to deposition in the Great Lakes region, it is difficult to trace emissions from point sources to impacted sites. Recent studies suggest that metal isotope ratios may be useful for distinguishing between and tracing source emissions. We measured Pb, strontium (Sr), and Hg isotope ratios in daily precipitation samples that were collected at seven sites across the Great Lakes region between 2003 and 2007. Lead isotope ratios ($^{207}Pb/^{206}Pb = 0.8062$ to 0.8554) suggest that Pb deposition was influenced by coal combustion and processing of Mississippi Valley-Type Pb ore deposits. Regional differences in Sr isotope ratios ($^{87}Sr/^{86}Sr = 0.70859$ to 0.71155) are likely related to coal fly ash and soil dust. Mercury isotope ratios ($\delta^{202}Hg = -1.13$ to 0.13‰) also varied among the sites, likely due to regional differences in coal isotopic composition, and fractionation occurring within industrial facilities and in the atmosphere. These data represent the first combined characterization of Pb, Sr, and Hg isotope ratios in precipitation collected across the Great Lakes region. We demonstrate the utility of multiple metal isotope ratios in parallel with traditional trace element multivariate statistical modeling to enable more complete pollution source attribution.

1. Introduction

The emission and deposition of hazardous trace metals such as mercury (Hg) and lead (Pb) are of significant concern because they can affect human and environmental health (Clarkson et al., 2007; Evers et al., 2008; Laraque and Trasande, 2005). These metals are potent neurotoxins and are especially harmful to developing fetuses and young children (Clarkson et al., 2007; Laraque and Trasande, 2005). In fact, due to high fish methylmercury concentrations, all water bodies in the Great Lakes region currently have fish consumption advisories (U.S. EPA, 2009). Significant research has been devoted to understanding the sources, transport, deposition, and impacts of these metals in the region (Flegal et al., 1989; Hall et al., 2005; Keeler and Dvonch, 2005; Landis and Keeler, 2002; Landis et al., 2002; Risch et al., 2012).

Atmospheric deposition is a primary source of metals such as Hg to ecosystems in the Great Lakes region (Fitzgerald et al., 1991; Landis

Abbreviations: MVT, Mississippi Valley-Type; NIST, National Institute of Standards and Technology; SRM, standard reference material; MDF, mass-dependent fractionation; MIF, mass-independent fractionation; GEM, gaseous elemental mercury; GOM, gaseous oxidized mercury; PBM, particle bound mercury; UMAQL, University of Michigan Air Quality Laboratory; ICP-HRMS, inductively coupled plasma high resolution mass spectrometry; PMF, positive matrix factorization; HYSPLIT, hybrid single-particle Lagrangian integrated trajectory; MC-ICP-MS, multi-collector inductively coupled plasma mass spectrometry.

* Corresponding author. Tel.: +1 607 592 3026.
E-mail address: lsaylors@umich.edu (L.S. Sherman).

http://dx.doi.org/10.1016/j.scitotenv.2014.09.034
0048-9697/

and Keeler, 2002). Research over the last two decades has shown that local and regional sources (especially in the Chicago, Illinois and Detroit, Michigan urban and industrial areas) contribute significantly to this deposition (Flegal et al., 1989; Gratz et al., 2013a; Keeler and Dvonch, 2005; Landis et al., 2002). Mercury is emitted to the atmosphere in the U.S. primarily by coal combustion, metal processing, waste incineration, and chemical and cement production (Pacyna et al., 2006; Pirrone et al., 2010). Similarly, major U.S. anthropogenic sources of Pb are coal and oil combustion, metal mining and processing, battery recycling, and oil refining (Graney and Landis, 2013; Komárek et al., 2008; Nriagu and Pacyna, 1998). Previous studies have estimated source contributions using a variety of methods including measurement of metals in precipitation (Glass and Sorensen, 1999; Gratz et al., 2009; Keeler et al., 2005, 2006; White et al., 2009), meteorological analyses (Cohen et al., 2004, 2007; Dvonch et al., 2005; Landis and Keeler, 2002), and multivariate statistical receptor modeling (Gratz and Keeler, 2011; Gratz et al., 2013b; Keeler et al., 2006). However, due to complex atmospheric chemistry, transport patterns, meteorological conditions, the mixing of emissions from multiple sources, and uncertainties associated with receptor modeling, it remains difficult to quantify the relative impact of emissions from different sources on metal deposition.

Radiogenic isotope ratios of metals such as Pb and strontium (Sr) are not measurably modified by industrial, atmospheric, or environmental processes and can be used to characterize emissions from different sources (Geagea et al., 2007; Graney and Landis, 2013; Grousset and Biscaye, 2005; Simonetti et al., 2000a, 2000b). For several decades, Pb isotope ratios measured in ice cores, snow, weekly-integrated precipitation, aerosols, soils, and lichens have been used to distinguish between deposition resulting from leaded gasoline combustion, metal smelters, coal-fired power plants, and waste incinerators (DesJardins et al., 2004; Erel et al., 1997; Geagea et al., 2007; Haack et al., 2002; Kaste et al., 2003; Rabinowitz and Wetherill, 1972; Simonetti et al., 2000b, 2000c; Sturges and Barrie, 1987, 1989; Sturges et al., 1993). However, source–receptor relationships can be determined most accurately by analyzing short-term daily samples (Dvonch et al., 1999; Graney and Landis, 2013; Gratz et al., 2010; Hoyer et al., 1995) or sub-daily event-based samples (White et al., 2009, 2013). A recent study in the Great Lakes region used Pb isotope ratios measured in daily precipitation samples in combination with air mass back trajectory analyses, and trace element concentrations to distinguish between anthropogenic Pb emission sources (Graney and Landis, 2013). In some cases, Sr isotope ratios have been used in conjunction with Pb isotope ratios to further constrain metal sources (Geagea et al., 2007; Grousset and Biscaye, 2005; Simonetti et al., 2000a, 2000b). In addition, methodological developments now allow the precise measurement of Hg isotopes in precipitation samples and recent studies suggest that Hg isotope ratios may be used to distinguish between emission sources (Chen et al., 2012; Gratz et al., 2010; Sherman et al., 2012; Sun et al., 2013).

The combination of multiple isotopic systems may ultimately improve source apportionment capabilities as well as allow characterization of the isotopic composition of atmospheric end-members for ecological studies of base cations (e.g., calcium, Ca) and metal (e.g., Hg and Pb) cycling in sensitive ecosystems (Bailey et al., 1996; Blum et al., 2002; Demers et al., 2013; Erel et al., 1997; Kaste et al., 2003; Miller et al., 1993). Very little data exists with which to evaluate the metal isotopic variability of either atmospheric sources or deposition in the Midwestern U.S. For example, although several previous studies have used Sr isotope ratios as a proxy tracer for Ca transport through forest ecosystems, these studies relied on a limited number of Sr isotope ratio measurements in precipitation (e.g., Bailey et al., 1996; Blum and Erel, 1997; Blum et al., 2002; Miller et al., 1993). We conducted this study both to characterize the values and variability of Pb, Sr, and Hg isotope ratios in precipitation in the Great Lakes region and to assess the hypothesis that multiple isotope systems can be used to improve metal source attribution estimates.

1.1. Lead, strontium, and mercury isotopes

There are four stable isotopes of Pb with the following approximate abundances: ^{208}Pb (52.4%), ^{207}Pb (24.1%), ^{206}Pb (22.1%), and ^{204}Pb (1.4%). ^{204}Pb is non-radiogenic and was not measured in this study because of its low relative abundance. ^{208}Pb, ^{207}Pb, and ^{206}Pb are formed by the radioactive decay of ^{232}Th (half-life = 14 billion years), ^{235}U (half-life = 0.7 billion years), and ^{238}U (half-life = 4.5 billion years), respectively. The ratios of these isotopes vary in geologic materials due to differences in the relative concentrations of the parent and daughter isotopes and the age of the rock or ore body. In the U.S., the primary Pb producing ores are Mississippi Valley-Type (MVT) lead–zinc–copper ores, which have distinctly lower ^{207}Pb/^{206}Pb ratios than most other ores (MVT ^{207}Pb/^{206}Pb = 0.714 to 0.781; Doe and Delevaux, 1972; Goldhaber et al., 1995; Heyl et al., 1974; Komárek et al., 2008). These distinct Pb isotope ratios have been used to identify MVT ore-derived Pb in U.S. leaded gasoline and metallurgical emissions (Bollhöfer and Rosman, 2001; Graney et al., 1995; Graney and Landis, 2013; Komárek et al., 2008; Simonetti et al., 2000c; Sturges and Barrie, 1989). After the phase-out of leaded gasoline in the U.S. in the 1980s and 1990s and decreased primary Pb ore production (Herrick and Friedland, 1990; Shen and Boyle, 1987; Veron et al., 1993), the major U.S. sources of Pb to the atmosphere became more diverse and now include detectable emissions from facilities that recycle scrap metal from multiple sources (Rabinowitz, 2005; Sturges and Barrie, 1987).

Strontium is present in all Ca-bearing geologic materials including rocks, soils, and coals. There are four stable isotopes of Sr with the following approximate abundances: ^{88}Sr (82.6%), ^{87}Sr (7.0%), ^{86}Sr (9.9%), and ^{84}Sr (0.6%). Of these, only ^{87}Sr is radiogenic and forms by the radioactive decay of ^{87}Rb (half-life = 48.8 billion years). ^{87}Sr/^{86}Sr ratios are distinct in rocks of different ages and lithologies, as well as in soils, vegetation, and surface waters (Blum and Erel, 2003; Burke et al., 1982). Strontium is also present in coal and is concentrated in fly ash after combustion (Hurst and Davis, 1981; Hurst et al., 1991). Previous studies have used Sr isotopes to trace sources of airborne dust to soils and lake sediments, as well as fly ash leachates into ecosystems (Hurst et al., 1991, 1993; Miller et al., 1993; Simonetti et al., 2000c; Spivak-Birndorf et al., 2012; Stancin et al., 2006; Straughan et al., 1981). However, only a few studies have measured Sr isotope ratios in precipitation samples (e.g., Bailey et al., 1996; Blum and Erel, 1997; Bullen et al., 1996; Miller et al., 1993; Simonetti et al., 2000b, 2000c).

In contrast to Pb and Sr, Hg isotopes are non-radiogenic and isotopic variability is caused by fractionation during biogeochemical processes. There are seven stable isotopes of Hg with the following approximate abundances: ^{204}Hg (6.8%), ^{202}Hg (29.7%), ^{201}Hg (13.2%), ^{200}Hg (23.1%), ^{199}Hg (16.9%), ^{198}Hg (10.0%), and ^{196}Hg (0.2%). Mercury isotope ratios are reported using delta notation (Eq. (1)).

$$\delta^{xxx}\mathrm{Hg}\,(‰) = \left(\left[\left(^{xxx}\mathrm{Hg}/^{198}\mathrm{Hg}\right)_{\mathrm{sample}} / \left(^{xxx}\mathrm{Hg}/^{198}\mathrm{Hg}\right)_{\mathrm{SRM\ 3133}}\right] - 1\right) * 1000. \quad (1)$$

In Eq. (1), xxxHg is an isotope of Hg and SRM 3133 is the National Institute of Standards and Technology (NIST) Standard Reference Material (SRM) (Bergquist and Blum, 2007). Mercury isotopes can undergo mass-dependent fractionation (MDF) during a number of biotic and abiotic processes (Bergquist and Blum, 2007; Estrade et al., 2009; Kritee et al., 2007, 2009; Rodríguez-González et al., 2009; Zheng et al., 2007) and mass-independent fractionation (MIF) primarily during photochemical reactions (Bergquist and Blum, 2007; Buchachenko, 2001; Zheng and Hintelmann, 2010). Mass-independent fractionation is reported as the deviation of a measured

isotope ratio from the theoretically predicted ratio based on the MDF law (Eq. (2)).

$$\Delta^{xxx}Hg = \delta^{xxx}Hg - \left(\delta^{202}Hg * \beta\right). \quad (2)$$

In Eq. (2), β for kinetic reactions is equal to 0.252 for ^{199}Hg, 0.502 for ^{200}Hg, 0.752 for ^{201}Hg, and 1.493 for ^{204}Hg (Bergquist and Blum, 2007).

It is especially difficult to quantify Hg source–receptor relationships because emitted Hg can be transported globally as a reduced elemental gas (GEM) or deposited near sources as gaseous oxidized Hg (GOM) and particulate bound Hg (PBM) (Lin and Pehkonen, 1999; Schroeder and Munthe, 1998). Recent studies have begun to characterize Hg isotope ratios in source materials such as coals and other studies have begun to trace atmospheric Hg emissions using Hg isotopes (Biswas et al., 2008; Chen et al., 2012; Gratz et al., 2010; Lefticariu et al., 2011; Rolison et al., 2013; Sherman et al., 2012; Sun et al., 2013; Yin et al., 2013, 2014). Coals from North America, China, and Russia generally display negative δ^{202}Hg values (mean = −1.21‰, 1 SD = 0.64‰, n = 89) and slightly negative Δ^{199}Hg values (mean = −0.09‰, 1 SD = 0.15‰, n = 89) (Biswas et al., 2008; Lefticariu et al., 2011; Sherman et al., 2012; Sun et al., 2013; Yin et al., 2014). In addition to isotopic differences among combusted coals, fractionation of Hg isotopes occurs within coal-fired power plants. Sherman et al. (2012) observed extreme negative δ^{202}Hg values (<−3.0‰) in rainfall collected near a large coal-fired power plant in Florida. Subsequently, Sun et al. (2013, 2014) modeled Hg fractionation in two Chinese coal-fired power plants and found that the light isotopes of Hg were preferentially oxidized and absorbed onto fly ash whereas the heavy isotopes of Hg were preferentially emitted as GEM. It is therefore possible that near-field deposition of the oxidized Hg species (i.e., PBM and GOM) resulted in the negative δ^{202}Hg values observed in precipitation near the Florida power plant (Sherman et al., 2012). Although more research is needed to fully understand Hg isotope fractionation within industrial sources, these studies suggest that Hg isotope ratios may be used to identify emissions from sources such as coal-fired power plants.

2. Methods

2.1. Sample collection

Daily precipitation samples used in this study were collected between July 2003 and January 2007 at five sites in Michigan, one rural site in Vermont, and one site impacted by industrial emissions in Ohio (Fig. 1). The precipitation samples analyzed during this study represent a subset of the total collected samples. As shown in Fig. 1, these sites were located in proximity to a variety of local and regional emission sources including coal-fired power production, iron and steel production, non-ferrous metal processing, municipal waste and sewage incineration, and cement production. The precipitation collection sites in Michigan were operated by the University of Michigan Air Quality Laboratory (UMAQL) as part of a study to assess sources of Hg deposition (UMAQL, 2009). These sites included two southern Michigan urban locations: Grand Rapids (GRD; 42.9600N, 85.1491W) and southwest Detroit (FRT; 42.3030N, 83.1054W); one southern Michigan rural location: Dexter (DXT; 42.4167N, 83.9019W); and two northern Michigan rural locations: Eagle Harbor (EGL; 47.4596N, 88.1491W) and Pellston (PLN; 45.4487N, 84.6776W). The rural site at Underhill, Vermont was located ~25 km east of Lake Champlain (LCH; 44.5283N, 72.8684W) and was operated by UMAQL from 1992 to 2007 (Gratz et al., 2009; Keeler et al., 2005). The site impacted by industry at Steubenville, Ohio (STB; 40.3794N, 80.6195W) was operated through a cooperative agreement between the U.S. Environmental Protection Agency (U.S. EPA) and UMAQL from 2002 to 2007 (Keeler et al., 2006; White et al., 2009, 2013). This site was located in close proximity to numerous emission sources including five large coal-fired power plants within a 50 km radius, iron/steel and non-ferrous metal production facilities, slag processing, and incinerators (Keeler et al., 2006; Vedantham et al., 2014; White et al., 2009). Previous studies identified elevated Hg deposition at this site (Keeler et al., 2006; White et al., 2009) as well as high concentrations of other hazardous air pollutants, including particulate matter (Dockery et al., 1993; Vedantham et al., 2014).

Daily wet-only precipitation samples were collected as described previously using modified wet-only automatic collectors (MIC-B; Landis and Keeler, 1997). Each collector had separate acid-cleaned glass/Teflon sampling trains for Hg samples and polypropylene sampling trains for trace element samples (Gratz and Keeler, 2011; Gratz et al., 2009; Keeler et al., 2006; Landis and Keeler, 2002). After collection, trace element samples were acidified with trace metal-grade HNO_3 to a concentration of 0.2% (v/v) and metal concentrations were measured by inductively coupled plasma high resolution mass spectrometry (ICP-HRMS; Thermo Scientific Element2) as reported previously (UMAQL, 2009; Gratz and Keeler, 2011; Keeler et al., 2006; White, 2009). Previous research has demonstrated that metals, including Pb, are stable in acidified precipitation samples stored in polypropylene bottles for at least ten years (Graney and Landis, 2013). After collection, Hg samples were oxidized with Hg-free BrCl to a concentration of 1% (v/v) as reported previously (UMAQL, 2009; Gratz and Keeler, 2011; Keeler et al., 2006; White et al., 2009). The original Teflon sampling bottles were tightly closed, sealed with Teflon tape, double bagged, and stored in a dark cold-room. We expect that oxidized precipitation samples stored under these conditions should be stable and fully retain Hg for many years (Parker and Bloom, 2005).

A subset of samples was chosen for isotopic analysis based on sample availability, adequate Hg mass, and collection date to provide maximal seasonal coverage. Because emissions from nearby sources may result in higher localized metal deposition (White et al., 2013), this data set may be biased toward the identification of local and regional emission sources. In total, 32 precipitation samples were analyzed for Pb, Sr, and Hg isotope ratios (Table 1). Due to sample availability and/or low metal concentrations, 26 other samples were analyzed for only one or two of the three isotope systems investigated (Table 1).

2.2. Previous analyses

Positive Matrix Factorization (PMF) is an advanced mathematical receptor modeling tool implemented by the U.S. EPA that utilizes a matrix of trace element concentrations to retrospectively identify contributing atmospheric pollution sources by the presence of unique elemental tracers that have a significant influence on the modeled data set (U.S. EPA, 2014; Paatero, 1997). Mesoscale meteorological air mass back trajectories calculated using the NOAA Hybrid Single-Particle Lagrangian Integrated Trajectory (HYSPLIT) model (Draxler and Rolph, 2010) can be paired with these quantitative source estimates. Using PMF, previous studies identified up to six sources that impacted metal deposition at the Great Lakes collection sites (UMAQL, 2009; Gratz and Keeler, 2011; Keeler et al., 2006; White et al., 2009). According to these analyses, Hg deposition at these sites is largely attributable to coal combustion (61–83% of total accounted for Hg deposition) whereas Pb deposition is attributable primarily to smelter and incinerator emissions (51–73% of total accounted for Pb deposition) and secondarily to coal combustion (<5%–40% of total accounted for Pb deposition) (UMAQL, 2009; Gratz and Keeler, 2011; Keeler et al., 2006; White et al., 2009). Rural sites such as Dexter, Michigan, and Underhill, Vermont, are impacted by regional Hg emissions from coal combustion and other sources that are transported from Midwestern urban and industrial centers such as Chicago, Detroit, and the Ohio River Valley (Gratz and Keeler, 2011; Liu et al., 2010). In contrast, Hg wet deposition at the Steubenville, Ohio site is dominantly impacted by local coal combustion and metal processing (Keeler et al., 2006; White et al., 2009, 2013).

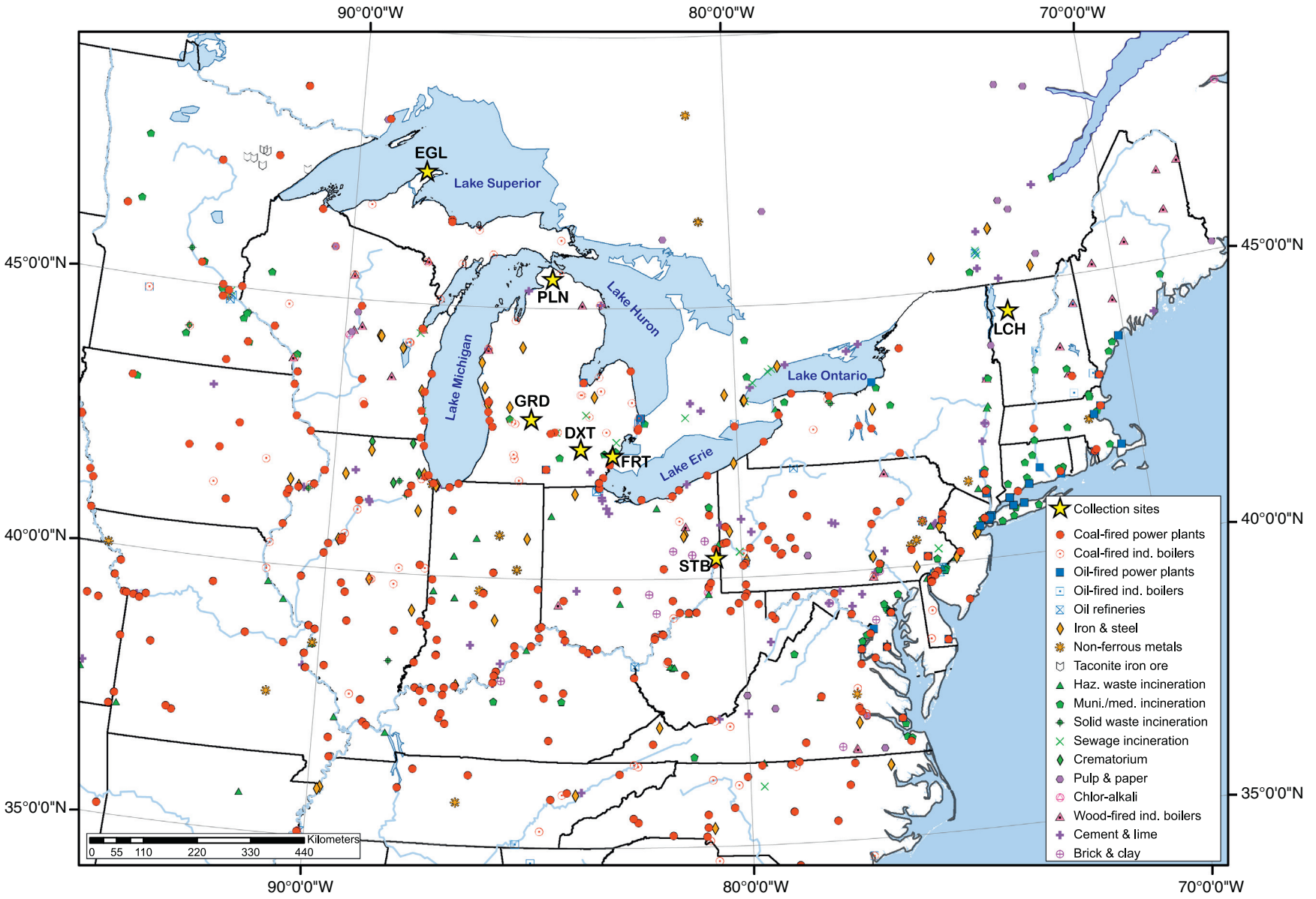

Fig. 1. Map of precipitation collection sites and sources in the Great Lakes region. Depicted sources are those that emitted >1 kg of Hg per year in 2005 as reported in the U.S. EPA National Emissions Inventory and Environment Canada National Pollutant Release Inventory (U.S. EPA, 2005; NPRI, 2008). Collection sites are marked with yellow stars and sources are depicted using symbols as indicated in the legend. Site name abbreviations are as follows: Detroit, Michigan (FRT), Dexter, Michigan (DXT), Eagle Harbor, Michigan (EGL), Grand Rapids, Michigan (GRD), Pellston, Michigan (PLN), Steubenville, Ohio (STB), and Underhill, Vermont (LCH). (For interpretation of the references to color in this figure legend, the reader is referred to the web version of this article.)

Table 1
Abbreviated isotope results for precipitation samples. Collection site abbreviations are as follows: Detroit, Michigan (FRT), Dexter, Michigan (DXT), Eagle Harbor, Michigan (EGL), Grand Rapids, Michigan (GRD), Pellston, Michigan (PLN), Steubenville, Ohio (STB), and Underhill, Vermont (LCH). Analytical uncertainties for the measured $^{87}Sr/^{86}Sr$ ratios (2SE) represent error in the last two or three presented decimal places. Ratios that were not measured due to low metal concentrations are listed as "n.d." Samples that were collected but not archived for future analyses and could not be analyzed are listed as "sample not retained".

Precipitation date	Site ID	Sample ID	$\delta^{202}Hg$ (‰)	$\Delta^{199}Hg$ (‰)	$^{207}Pb/^{206}Pb$	$^{208}Pb/^{206}Pb$	$^{87}Sr/^{86}Sr \pm 2SE$
07/04/04	DXT	741	−0.35	0.36	0.8438	2.0620	0.710081 ± 35
07/12/04	DXT	742	−0.51	0.29	0.8421	2.0541	0.709807 ± 29
01/12/05	DXT	775	Sample not retained		0.8404	2.0581	0.708924 ± 32
06/13/05	DXT	803	sample not retained		0.8490	2.0674	0.710721 ± 55
07/24/05	DXT	816	Sample not retained		0.8339	2.0449	0.710415 ± 36
09/22/05	DXT	826	Sample not retained		0.8336	2.0435	0.709850 ± 31
05/14/05	EGL	683	Sample not retained		0.8511	2.0728	n.d.
06/23/05	EGL	692	Sample not retained		0.8386	2.0482	0.709669 ± 24
06/28/05	EGL	693	Sample not retained		0.8497	2.0753	0.710208 ± 40
07/27/03	FRT	23	−0.50	−0.20	0.8266	2.0344	0.709004 ± 25
08/02/03	FRT	24	0.03	−0.87	0.8360	2.0460	0.708753 ± 26
06/09/04	FRT	99	0.10	0.19	0.8310	2.0409	0.708610 ± 28
05/13/05	FRT	206	Sample not retained		0.8294	2.0417	0.708773 ± 78
11/02/03	GRD	135	0.07	0.24	0.8413	2.0602	0.708891 ± 62
05/21/04	GRD	182	−0.06	0.40	0.8423	2.0608	0.709303 ± 26
05/30/04	GRD	183	0.02	0.51	0.8445	2.0663	0.709818 ± 24
10/23/04	GRD	215	−0.17	0.14	0.8411	2.0569	0.708591 ± 30
01/13/05	GRD	234	Sample not retained		0.8322	2.0452	0.709155 ± 30
03/30/05	GRD	244	Sample not retained		0.8062	1.9917	0.709286 ± 19
05/13/05	GRD	251	−0.05	0.46	0.8430	2.0610	0.709087 ± 42
06/05/05	GRD	256	Sample not retained		0.8386	2.0497	0.709465 ± 25
06/30/05	GRD	262	Sample not retained		0.8331	2.0427	0.709659 ± 24
07/23/05	GRD	267	−0.12	0.52	0.8345	2.0486	0.709986 ± 44
09/22/05	GRD	278	−0.07	0.27	0.8336	2.0433	0.710371 ± 33
11/05/05	GRD	288	0.09	0.33	0.8402	2.0566	0.709243 ± 35
11/09/05	GRD	289	Sample not retained		0.8366	2.0452	0.708992 ± 23
10/02/06	GRD	352	−0.06	0.51	0.8331	2.0466	0.710463 ± 27
8/04–06/03	LCH	163	−0.47	−0.13	Sample not retained		
10/20–21/03	LCH	180	0.07	0.36	Sample not retained		
07/01/04	LCH	264	−0.06	0.16	0.8472	2.0649	0.710322 ± 41
8/12–13/04	LCH	280	−0.17	0.99	Sample not retained		
07/05/05	LCH	368	−0.15	−0.09	0.8480	2.0788	0.709348 ± 25
08/31/05	LCH	382	−0.20	0.42	0.8505	2.0562	0.710083 ± 43
09/17/05	LCH	385	Sample not retained		0.8493	2.0686	0.710282 ± 34
04/19/04	PLN	428	0.13	0.66	0.8439	2.0687	0.710122 ± 24
05/23/04	PLN	436	−0.07	0.35	0.8543	2.0937	0.710397 ± 35
08/09/05	PLN	500	Sample not retained		0.8338	2.0447	0.710107 ± 32
08/19/05	PLN	502	−0.31	0.15	0.8480	2.0691	0.710112 ± 47
05/11/06	PLN	534	−0.08	0.11	0.8438	2.0649	n.d.
06/14/04	STB	141	Recovery <80%		0.8554	2.0825	0.709959 ± 24
08/19/04	STB	157	−0.30	0.85	0.8299	2.0324	0.709702 ± 33
8/28–30/04	STB	159	−0.37	0.74	0.8425	2.0531	0.710496 ± 28
09/08/04	STB	160	−0.68	0.51	0.8252	2.0267	0.711469 ± 43
01/11/05	STB	177	−0.68	0.05	0.8249	2.0140	0.709678 ± 50
02/09 & 02/14/05	STB	180	−1.13	−0.14	0.8088	1.9591	0.71051 ± 37
03/28/05	STB	186	−0.60	0.33	0.8390	2.0573	0.709951 ± 58
04/02/05	STB	187	−0.63	0.14	Sample not retained		
04/20/05	STB	188	−0.09	0.48	Sample not retained		
05/13/05	STB	190	−0.37	0.41	0.8363	2.0510	0.710468 ± 31
06/28/05	STB	198	−0.50	−0.14	0.8349	2.0457	0.711553 ± 34
06/30/05	STB	200	−0.34	0.07	0.8332	2.0385	0.710435 ± 101
07/26/05	STB	212	Sample not retained		0.8440	2.0552	0.710781 ± 21
10/23/05	STB	230	Sample not retained		0.8376	2.0498	0.710633 ± 97
11/14/05	STB	236	−0.80	0.02	0.8496	2.0689	0.710597 ± 65
01/02/06	STB	245	−0.63	0.19	0.8393	2.0567	0.710140 ± 22
04/21/06	STB	266	−0.15	0.28	Sample not retained		
06/22/06	STB	275	−0.14	0.73	0.8438	2.0583	0.710287 ± 36
01/05/07	STB	322	−0.07	0.09	n.d.	n.d.	0.710036 ± 35

2.3. Isotopic analyses: lead

The selected precipitation samples were measured for Pb isotope ratios without pre-concentration or column separation using ICP-HRMS following previously described methods (Graney and Landis, 2013). Lead isotopic standard NBS 981 was used to correct for internal mass bias using standard-sample bracketing with Pb concentrations matched to within 10%. All samples with Pb concentrations >1 μg/L were diluted to 1 μg/L. Two secondary standards, BCR-2 and TMRAIN-95, and 1% HNO_3 blanks were analyzed with each block of five samples. BCR-2 is a rock standard that was hot acid digested (Stancin et al., 2006) and diluted in 1% HNO_3 to concentrations ranging from 0.1 to 1 μg/L. TMRAIN-95 is a synthetic rainfall standard that was analyzed at 0.3 μg/L. Measured Pb isotope ratios for the BCR-2 standard across all sample concentrations were within error of reported values (this study: mean $^{207}Pb/^{206}Pb$ = 0.8333, 2 SD =

0.0042, n = 19, mean $^{208}Pb/^{206}Pb$ = 2.0658, 2 SD = 0.0065, n = 19; Weis et al., 2006: mean $^{207}Pb/^{206}Pb$ = 0.8332, 2 SD = 0.0009, n = 11, mean $^{208}Pb/^{206}Pb$ = 2.0649, 2 SD = 0.0004, n = 11). Measured analytical uncertainties for the TMRAIN-95 standard were similar to those for BCR-2 (mean $^{207}Pb/^{206}Pb$ = 0.8138, 2 SD = 0.0040, n = 19; mean $^{208}Pb/^{206}Pb$ = 2.0032, 2 SD = 0.0097, n = 19). Lead isotope ratios measured in sample replicates (n = 11) at all concentrations were the same within the reported uncertainties (see Appendix A). Blank intensities remained constant throughout the analytical session and represented an average of 1.1 ± 0.9% (1 SD, range = 0.2–6.7%) of the sample ^{208}Pb signal intensity. Blank correction did not significantly change the Pb isotope ratios and the reported data were not blank corrected.

2.4. Isotopic analyses: strontium

Splits of the precipitation samples (15–240 mL, 20–230 ng of Sr) were filtered to 0.45 μm using acid-cleaned filters (n = 50) to avoid any interference in the column separation of Sr by particulates. A replicate subset of samples (n = 5) analyzed without filtration did not display significant differences in Sr isotope ratios (see Appendix B). Where possible, enough sample was filtered to obtain >50 ng of Sr. The samples were then evaporated to dryness on a hot plate at 80 °C and reconstituted in 0.5 mL of ultrapure 3N HNO_3. Strontium was separated from the matrix by cation exchange chromatography using columns packed with Sr-specific resin (Eichrom Sr-Spec) as described previously (Stancin et al., 2006). After the samples were loaded on the columns, matrix elements were eluted in 2.9 mL of 3N HNO_3 and Sr was eluted in 2 mL of 0.05N HNO_3. The samples were then evaporated to dryness and loaded onto tungsten filaments in 1 μL of 1N HCl. Strontium isotope standards (NBS 987) and deionized water blanks were processed in the same manner. Procedural blanks contained <1% of the average sample Sr mass and were thus negligible (mean Sr blank = 0.38 ng, 1 SD = 0.09 ng, n = 4).

Strontium isotope ratios were measured by thermal ionization mass spectrometry (Finnigan MAT 262) according to previously published methods (Stancin et al., 2006). The $^{87}Sr/^{86}Sr$ ratios were corrected for internal mass bias to an $^{86}Sr/^{88}Sr$ ratio of 0.1194. During the analysis period for this study (October 2013–January 2014), the measured mean $^{87}Sr/^{86}Sr$ ratio for NBS 987 was 0.71022 ± 0.000024 (2 SD, n = 26).

2.5. Isotopic analyses: mercury

Prior to isotopic analyses, Hg concentrations were measured in the precipitation samples using atomic absorption spectrometry (see Appendix B). Mercury in the precipitation samples was then separated and concentrated according to previously described methods (Demers et al., 2013; Sherman et al., 2012). Briefly, samples (266–977 mL in volume) were diluted to a volume of 1 L with 1% BrCl (v/v) and neutralized with 0.3 mL of 30% $NH_2OH \cdot HCl$ (w/w). Ten percent $SnCl_2$ (w/w) was then slowly added to each sample through a three-port cap. The resulting GEM was pulled into acidic 1% $KMnO_4$ (w/w) solutions using a vacuum pump. Procedural standards (n = 6) and blanks (n = 1) were processed in the same manner. Mercury in procedural standards consistently had high recovery in the final solutions (mean = 98%, 1 SD = 6%, n = 6). With the exception of one sample, all of the samples also had high recovery after separation and concentration (84–120%, mean = 101%, 1 SD = 8%, n = 40; Appendix C). For unknown reasons, one sample (STB 141) had lower recovery (77%) and was, therefore, excluded from the data set.

Mercury isotopic compositions were measured in the concentrated sample and standard solutions using continuous-flow cold vapor generation multi-collector inductively coupled plasma mass spectrometry (MC-ICP-MS; Nu Instruments Nu plasma) according to previously published methods (Blum and Bergquist, 2007). The UM-Almadén secondary standard was analyzed at least five times in each analytical session. Maximum sample analytical uncertainty is estimated as the greater of the 2 SD variability of a given isotope ratio measured in the procedural standards or in the UM-Almadén secondary standard. Analytical uncertainty was observed to increase at concentrations <2 μg/L. Because many of the samples in this study were analyzed at concentrations <2 μg/L (0.9–1.9 μg/L, n = 26), uncertainties were calculated for UM-Almadén secondary standards analyzed both at <2 μg/L (0.8–1.9 μg/L) and ≥2 μg/L (2.0–5.0 μg/L) (Appendix C).

2.6. Meteorological analyses

In addition to Pb, Sr, and Hg isotope ratios, and previous PMF receptor modeling, we explored the meteorology associated with each precipitation event. We utilized HYSPLIT back trajectories (Draxler and Rolph, 2010) that were made publically available online by the University of Michigan Department of Atmospheric, Ocean, and Space Science (University of Michigan, 2012). These trajectories were calculated every 6 h starting at 500 m using EDAS40 data from the National Weather Service (40 km, 3 h resolution). Surface meteorological maps and atmospheric sounding data were used to characterize frontal systems, surface wind directions, and vertical stability (National Weather Service and Colorado State University, 2014; University of Wyoming, 2014).

2.7. Statistical analyses

Statistical significance was assessed using SAS 9.4 statistical analysis software (SAS Institute Inc., 2013). Wilcoxon non-parametric tests were conducted using the NPAR1WAY procedure utilizing the exact option to calculate *p*-values based on linear rank statistics. These tests were used to compare $^{207}Pb/^{206}Pb$ ratios between samples collected at rural and urban/impacted sites, $^{87}Sr/^{86}Sr$ ratios between samples collected in Steubenville and Grand Rapids/Detroit and $\delta^{202}Hg$ values between samples collected in Steubenville and Grand Rapids.

3. Results and discussion

3.1. Lead isotope ratios

Abbreviated isotopic results are presented in Table 1 and complete data are presented in Appendix C. Measured Pb isotope ratios in the precipitation samples are shown in Fig. 2A–B along with previous measurements of North American coals (Chow and Earl, 1972; Díaz-Somoano et al., 2009), MVT ores (Doe and Delevaux, 1972; Goldhaber et al., 1995; Heyl et al., 1974), and recent precipitation samples from the Great Lakes region (i.e., post 1990) (Graney and Landis, 2013; Simonetti et al., 2000c). Precipitation samples collected during this study displayed similar Pb isotope ratios to those of previously analyzed precipitation samples and North American coals (Fig. 2A–B). There were significant differences between precipitation samples collected at the rural sites (Fig. 2A) and those collected at the urban/industrial sites (Fig. 2B) ($Z = 3.4992$, $p < 0.0001$). Precipitation samples collected at the rural sites (DXT, EGL, LCH, and PLN) displayed less Pb isotopic variability and significantly higher $^{207}Pb/^{206}Pb$ ratios (Fig. 2A; $^{207}Pb/^{206}Pb$: 0.8336 to 0.8543, mean = 0.8445, 1 SD = 0.0063, n = 18) than samples collected at the urban/industrial sites (FRT, GRD, and STB; Fig. 2B; $^{207}Pb/^{206}Pb$: 0.8062 to 0.8554, mean = 0.8345, 1 SD = 0.0098, n = 33). These differences may be due to the variable influence of local Pb sources at the urban/industrial sites in contrast with more consistent, regionally-sourced Pb deposition at the rural sites (Graney and Landis, 2013). For example, in some cases, the lower $^{207}Pb/^{206}Pb$ ratios measured in precipitation collected at the urban/industrial sites may be due to the influence of emissions from MVT ore processing (see Section 3.4.1).

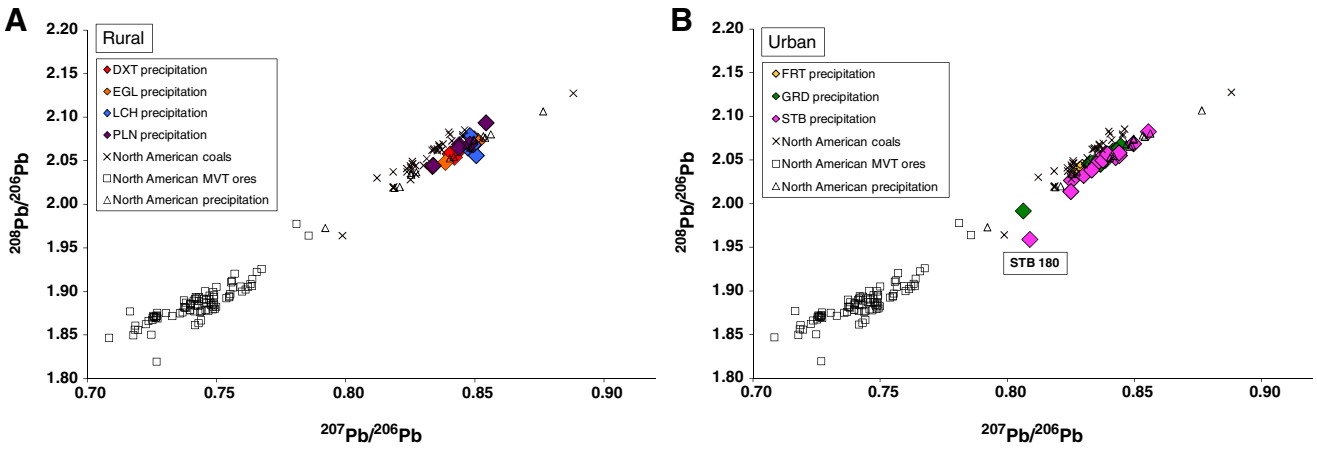

Fig. 2. Pb isotope ratios in precipitation samples and sources. Previously published analyses of North American coals are shown as x's (Chow and Earl, 1972; Díaz-Somoano et al., 2009), North American MVT Pb ores are shown as open black squares (Doe and Delevaux, 1972; Goldhaber et al., 1995; Heyl et al., 1974), and precipitation samples collected in the Great Lakes region after 1990 are shown as open black triangles (Graney and Landis, 2013; Simonetti et al., 2000c). Precipitation samples collected at rural (Fig. 2A: DXT, EGL, LCH, and PLN) and urban sites (Fig. 2B: FRT, GRD, and STB) are shown as colored diamonds. Case study sample STB 180 is labeled (see Section 3.4). In both plots, analytical uncertainty (2 SD) for precipitation samples based on measurement of the BCR-2 and TMRAIN-95 standards is less than the size of the symbols. Site name abbreviations are as follows: Detroit, Michigan (FRT), Dexter, Michigan (DXT), Eagle Harbor, Michigan (EGL), Grand Rapids, Michigan (GRD), Pellston, Michigan (PLN), Steubenville, Ohio (STB), and Underhill, Vermont (LCH). (For interpretation of the references to color in this figure legend, the reader is referred to the web version of this article.)

3.2. Strontium isotope ratios

Precipitation samples analyzed during this study were characterized by $^{87}Sr/^{86}Sr$ ratios between 0.70859 and 0.71155 (Table 1, Fig. 3). These values are generally higher than those measured previously in precipitation collected in Montreal, Canada (Simonetti et al., 2000c), but similar to those measured in precipitation collected in the northeastern U.S. (Bailey et al., 1996; Blum et al., 2002; Miller et al., 1993). As shown in Fig. 3, there is a significant division in Sr isotopic composition between samples collected in Steubenville, Ohio and those collected in Grand Rapids, Michigan and Detroit, Michigan ($Z = 4.2267$, $p < 0.0001$). The Steubenville samples displayed significantly higher $^{87}Sr/^{86}Sr$ ratios (mean = 0.71042, 1 SD = 0.00054, n = 16) than those collected at the urban sites in Michigan (GRD: mean = 0.70945, 1 SD = 0.00055, n = 14; FRT: mean = 0.70879, 1 SD = 0.00016, n = 4). There are at least two possible contributing explanations for these differences: (i) suspended soil dust (and possibly sea-spray aerosol) impacting these sites displays regionally variable $^{87}Sr/^{86}Sr$ ratios or (ii) coal combustion in each region produces fly ash that has differing $^{87}Sr/^{86}Sr$ ratios.

During the last glacial maximum, all of the precipitation collection sites except for Steubenville were glaciated. As a result, soils in the Grand Rapids and Detroit areas are relatively young and derived from glacial sediments, which are a mixture of Canadian Shield and Michigan Basin materials (Dreimanis and Goldthwait, 1973). In contrast, Steubenville is located ~50 km south of the furthest extent of glaciation (Hedman et al., 2009). Soils in the Steubenville area are more deeply weathered and derived from the local underlying bedrock, which consists of Pennsylvanian through Permian shales, siltstones, sandstones,

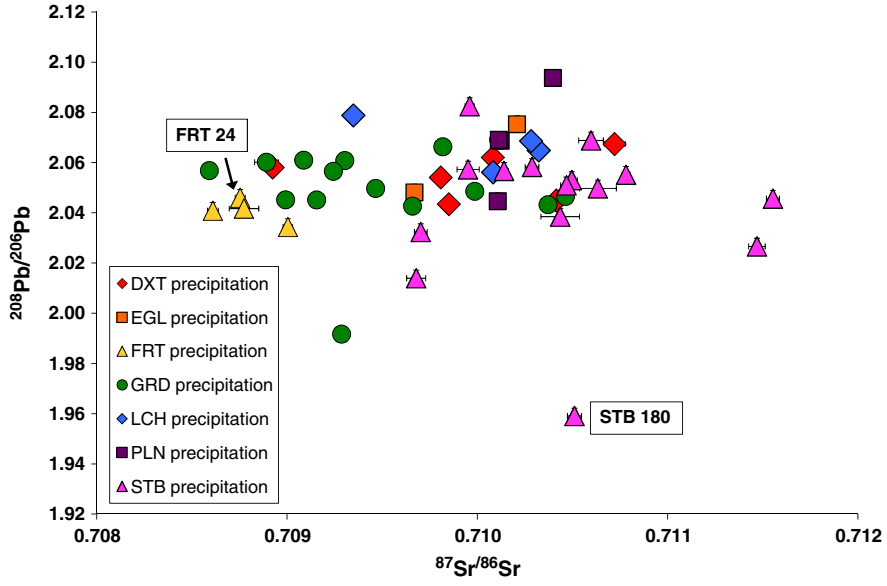

Fig. 3. $^{87}Sr/^{86}Sr$ versus $^{208}Pb/^{206}Pb$ in precipitation samples. Precipitation samples are shown using colored symbols by collection site. Case study samples FRT 24 and STB 180 are labeled (see Section 3.4). Analytical uncertainties for $^{87}Sr/^{86}Sr$ ratios (2 SD) are shown as error bars. Analytical uncertainty for $^{208}Pb/^{206}Pb$ ratios (2 SD) based on measurement of the BCR-2 and TMRAIN-95 standards is less than the size of the symbols. Site name abbreviations are as follows: Detroit, Michigan (FRT), Dexter, Michigan (DXT), Eagle Harbor, Michigan (EGL), Grand Rapids, Michigan (GRD), Pellston, Michigan (PLN), Steubenville, Ohio (STB), and Underhill, Vermont (LCH). (For interpretation of the references to color in this figure legend, the reader is referred to the web version of this article.)

and limestones (Brockman, 1998). It is possible that the older, bedrock-derived soils in the Steubenville area display different $^{87}Sr/^{86}Sr$ ratios than the younger glacially-derived soils in the Grand Rapids and Detroit areas. However, if soil isotopic composition was the primary factor controlling the observed differences in precipitation $^{87}Sr/^{86}Sr$ ratios, we might expect to observe similar $^{87}Sr/^{86}Sr$ ratios across all of the glaciated sites in Michigan. Instead, precipitation collected in Pellston and Eagle Harbor displayed $^{87}Sr/^{86}Sr$ ratios that were more similar to those observed in Steubenville, while precipitation collected in Dexter displayed seasonally variable $^{87}Sr/^{86}Sr$ ratios (see Appendix B). Similarly, the lack of correlation between $^{87}Sr/^{86}Sr$ ratios in precipitation with collection site distance from the Atlantic Coast suggests that the abundance of sea-spray aerosol (modern ocean $^{87}Sr/^{86}Sr = 0.7092$; DePaolo and Ingram, 1985; Hodell et al., 1990; McArthur et al., 2001; McArthur et al., 2006) was not a controlling factor of measured $^{87}Sr/^{86}Sr$ ratios.

We suggest that it is likely that fly ash emitted by coal-fired power plants and locally-deposited in Michigan and Ohio exhibits differing $^{87}Sr/^{86}Sr$ ratios. Strontium is present in coals in relatively low concentrations (Swaine, 1990), but is concentrated as a component in fine-particulate fly ash, reaching concentrations of up to 3000 μg/g (Hurst and Davis, 1981; Hurst et al., 1991; Straughan et al., 1981). Most coal-fired power plants in the U.S., including those located near Grand Rapids and Steubenville, use electrostatic precipitators to remove particulates from the flue gas stream (Brown et al., 1999). Although electrostatic precipitators remove ~80% of the fine particulate matter in the flue gas, U.S. power plants emitted an estimated ~68,000 Mg of fine particulates in 2005 (U.S. EPA, 2008; Clack, 2012). From 2004 to 2005, coal-fired power plants in Ohio purchased Appalachian Basin bituminous coal primarily from Ohio (45%), West Virginia (24%), and Kentucky (21%) (U.S. EIA, 2004–2005). In contrast, during the same time period, coal-fired power plants in Michigan purchased mainly sub-bituminous Powder River Basin (PRB) coal from Wyoming (47%) and Montana (28%) (U.S. EIA, 2004–2005). Carboniferous Appalachian Basin coals from Ohio, West Virginia, and Kentucky formed in coastal swamps and deltas (~300 Ma) (Heckel, 1995). In contrast, the much younger Paleogene PRB coals from Wyoming and Montana formed in brackish inland seas and swamps (~60 Ma) (Flores and Hanley, 1984). Due to their different depositional environments, composition, rank, and ages, coals from these two regions likely have differing Sr isotope ratios. However, only a limited number of studies have measured Sr isotope ratios in coals and fly ash (Hurst et al., 1991, 1993; Spivak-Birndorf et al., 2012). A recent study found that fly ash from U.S. sub-bituminous coals displayed lower $^{87}Sr/^{86}Sr$ ratios (mean = 0.71121, 1 SD = 0.00088, n = 5) than fly ash from U.S. bituminous coals (mean = 0.71309, 1 SD = 0.00075, n = 3) (Spivak-Birndorf et al., 2012). These data do not necessarily represent the full range of Sr isotope ratios displayed by U.S. coals or coals combusted in Michigan and Ohio. However, these data suggest that $^{87}Sr/^{86}Sr$ ratios vary systematically in coals depending on coal characteristics. It is therefore possible that sub-bituminous PRB coals combusted in Michigan may produce fly ash with lower $^{87}Sr/^{86}Sr$ ratios than the bituminous Appalachian Basin coals combusted in Ohio. If these isotopic differences are preserved in precipitation, they would be most easily observed at urban/industrial collection sites located near coal-fired power plants (i.e., Grand Rapids, Detroit, and Steubenville). The observed precipitation $^{87}Sr/^{86}Sr$ ratios in Grand Rapids, Detroit, and Steubenville may therefore have been influenced by the isotopic composition of locally-emitted fly ash.

3.3. Mercury isotope ratios

Great Lakes precipitation samples were generally characterized by negative $\delta^{202}Hg$ values (−1.13 to 0.13‰; Fig. 4), positive $\Delta^{199}Hg$ values (−0.20 to 0.99‰; Fig. 4), positive $\Delta^{200}Hg$ values (mean = 0.20‰, 1 SD = 0.08‰; see Appendix B), and negative $\Delta^{204}Hg$ values (mean = −0.36‰, 1 SD = 0.16‰; see Appendix B). With the exception of a few samples collected in Steubenville, the precipitation $\delta^{202}Hg$ values were similar to those observed previously in North American precipitation collected at sites impacted by mixed Hg emission sources (Chen et al., 2012; Demers et al., 2013; Donovan et al., 2013; Gratz et al., 2010; Sherman et al., 2012). Similarly, with the exception of one sample from Detroit that displayed an extreme negative $\Delta^{199}Hg$ value (−0.87‰; Table 1 and Fig. 4; see Section 3.4.2), the observed $\Delta^{199}Hg$ values were similar to those previously measured in precipitation (Chen et al., 2012; Demers et al., 2013; Donovan et al., 2013; Gratz et al., 2010; Sherman et al., 2012). It has been hypothesized that positive $\Delta^{199}Hg$ values in precipitation result from the preferential retention of the odd-mass-number isotopes of Hg in water droplets during photochemical reduction and loss of Hg (Chen et al., 2012; Gratz et al., 2010). It is likely that the MIF measured in the Great Lakes precipitation samples occurred due to similar photochemical processes (see Appendix B).

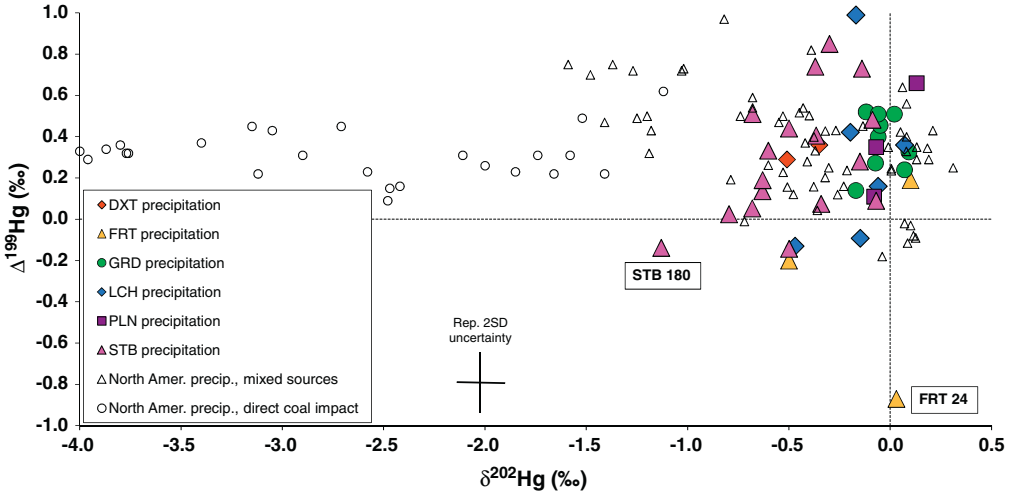

Fig. 4. $\delta^{202}Hg$ (‰) versus $\Delta^{199}Hg$ (‰) in precipitation samples. Precipitation samples are shown using colored symbols by collection site. Precipitation samples collected in North America at sites impacted by mixed sources are shown as open black triangles (Chen et al., 2012; Demers et al., 2013; Donovan et al., 2013; Gratz et al., 2010; Sherman et al., 2012), and precipitation samples directly impacted by a local coal-fired power plant are shown as open black circles (Sherman et al., 2012). Case study samples FRT 24 and STB 180 are labeled (see Section 3.4). Representative 2 SD analytical uncertainty based on analyses of procedural standards is shown. Site name abbreviations are as follows: Detroit, Michigan (FRT), Dexter, Michigan (DXT), Eagle Harbor, Michigan (EGL), Grand Rapids, Michigan (GRD), Pellston, Michigan (PLN), Steubenville, Ohio (STB), and Underhill, Vermont (LCH). (For interpretation of the references to color in this figure legend, the reader is referred to the web version of this article.)

Previous PMF estimates indicated that the majority of Hg deposition at all of the precipitation collection sites was attributable to coal combustion (UMAQL, 2009; Gratz and Keeler, 2011; Keeler et al., 2006; White et al., 2009). It is possible that the δ^{202}Hg values observed in these samples are related to the isotopic composition of combusted coal and fractionation occurring within coal-fired power plants. In a similar manner to Sr isotopes, the precipitation δ^{202}Hg values were significantly different between samples collected in Grand Rapids, Michigan and Steubenville, Ohio ($Z = 3.6834$, $p < 0.0001$). Samples collected in Grand Rapids displayed higher, less variable δ^{202}Hg values (mean = −0.04‰, 1 SD = 0.09‰, n = 9) than those collected in Steubenville (mean δ^{202}Hg = −0.47‰, 1 SD = 0.29‰, n = 16). This may be related to differences between the isotopic composition of PRB coal combusted in Michigan and Appalachian Basin coal combusted in Ohio. However, because only a limited number of PRB coals have been measured for Hg isotope ratios (Biswas et al., 2008), it is difficult to fully assess this possibility. It is also possible that Hg fractionation and removal within power plants, as well as proximity to power plants, results in the deposition of Hg with distinct δ^{202}Hg values in these two areas. As described above, Sun et al. (2013, 2014) modeled Hg fractionation within coal-fired power plants and found that emitted oxidized Hg species display more negative δ^{202}Hg values than emitted GEM. The Steubenville site was surrounded by coal-fired power plants, with the closest facility located ~15 km away and five facilities within a 50 km radius (Keeler et al., 2006; White et al., 2009). It is therefore possible that the more negative δ^{202}Hg values observed in samples collected at this site were caused by enhanced local deposition of PBM and GOM that displayed negative δ^{202}Hg values. Similarly, it is possible that the more positive δ^{202}Hg values observed in the Grand Rapids samples were a result of the oxidation and deposition of Hg that was emitted as GEM from non-local coal-fired power plants. Although there are no published experimental studies of Hg isotope fractionation during atmospheric oxidation of GEM, it is possible that this process may cause additional MDF of Hg isotopes such that the resulting oxidized species display higher δ^{202}Hg values. Because our current understanding of Hg fractionation within power plants and in the atmosphere is limited, we cannot conclusively evaluate these possibilities.

3.4. Precipitation case studies

3.4.1. Steubenville, Ohio: February 9 & February 14, 2005 (sample STB 180)

Although nearly all of the precipitation samples analyzed during this study represent an individual precipitation event, due to operator error, a few of the samples included integrated deposition from more than one discrete precipitating event. As a result, these multi-event samples may have been impacted by a wider variety of sources. This may dilute source-specific isotope ratios or trace element signatures, making source attribution more difficult.

A multi-event sample collected in Steubenville (sample STB 180) incorporated rain from two precipitation events: a short event on February 9, 2005 (16:00–24:00 UTC) and continuous rain on February 14, 2005 (2/14 10:00–2/15 4:00 UTC). The event on February 14 deposited substantially more rainfall (~22 mm) than the prior event (~6 mm) and was likely responsible for most of the metal deposition in this sample (White et al., 2009). Precipitation on February 14 was associated with a low-pressure system that moved across the Great Lakes and an accompanying cold front that passed over Ohio from west to east. Air mass transport to Steubenville in advance of the cold front was from the south. For 24 h prior to the event, southerly surface winds were light (<2 m/s) but these intensified during the event (5–6 m/s). As a result of these conditions, it is likely that local emissions from the coal-fired power plants and metallurgical processing facilities to the south of the Steubenville site (Vedantham et al., 2014; White et al., 2009) impacted deposition during this event.

Despite containing rainfall from more than one event, sample STB 180 exhibited distinct Pb and Hg isotope ratios (Figs. 2–4, Table 1). This sample displayed the lowest observed Pb isotope ratios (^{207}Pb/^{206}Pb = 0.8088, ^{208}Pb/^{206}Pb = 1.9591) and the most negative measured δ^{202}Hg value (−1.13 ± 0.13‰, 2 SD). In addition, PMF source attribution estimates for this sample were distinct in comparison to the other Steubenville samples (Fig. 5A–B) (White, 2009). As shown in Fig. 5, Pb deposition in Steubenville was generally dominated by emissions from coal combustion and incinerators/smelters while Hg deposition was dominated by coal combustion. In contrast, Pb and Hg deposition in sample STB 180 was impacted by coal combustion to a lesser degree relative to the other samples. Instead, Pb and Hg deposition in this sample was strongly influenced by scrap metal processing (Fig. 5). Using PMF, emissions from scrap metal processing near the Steubenville site have been identified as distinct from emissions related to metal smelters based on high concentrations of vanadium, chromium, and iron along with low zinc concentrations (White, 2009). The low Pb isotope ratios measured in sample STB 180 may indicate that these local scrap metal facilities processed metal that was originally mined as MVT Pb ores.

It is possible that Hg associated with these local scrap metal processing facilities displays more negative δ^{202}Hg values. This may be related either to the isotopic composition of the processed materials or fractionation occurring within the facilities. To date, no studies have measured Hg isotope fractionation within metallurgical facilities. However, Hg isotopes have been used to track Hg deposited to soils near metal smelters (Gray et al., 2013; Ma et al., 2013; Sonke et al., 2010). These soils generally display negative δ^{202}Hg values (mean = −0.99‰, 1 SD = 0.82‰, n = 104), suggesting that emissions from metal processing facilities may also display negative δ^{202}Hg values (Gray et al., 2013; Ma et al., 2013; Sonke et al., 2010).

It is also possible that enhanced deposition of PBM due to cold cloud processes could have resulted in the more negative δ^{202}Hg value observed in sample STB 180. Although precipitation during this event was composed of rain and not snow, cold cloud nucleation processes were likely dominant during February in Steubenville. During cold cloud processes, ice crystals can nucleate preferentially through heterogeneous processes involving crustal mineral particles (Baustian et al., 2012). Subsequent winter time precipitation results in significantly lower Hg deposition due to decreased within-cloud Hg scavenging (Burke et al., 1995; Hoyer et al., 1995). However, previous studies in the Great Lakes region have observed that winter ambient PBM concentrations are higher than in the summer and that ambient PBM concentrations are correlated with PBM concentrations in precipitation (Burke et al., 1995). As a result, winter samples collected in Steubenville likely contain more PBM emitted by local coal-fired power plants, which displays more negative δ^{202}Hg values. However, in general, there is no correlation among the Steubenville samples between δ^{202}Hg values and collection season.

3.4.2. Detroit, Michigan: July 27, 2003 (sample FRT 23) and August 2, 2003 (sample FRT 24)

The Detroit, Michigan precipitation collection site was located in southwest Detroit (Fig. 1). This site was heavily influenced by emissions from nearby truck traffic and industrial sources including coal-fired power plants, oil refineries, coke ovens, iron and steel production facilities, and a large sewage sludge incinerator (Keeler and Dvonch, 2005). Many of these facilities were located within 4 km of the collection site to the south and southwest (Liu et al., 2007).

Precipitation on July 27, 2003 (21:00–22:00 UTC; sample FRT 23) was the result of a low-pressure system over Ontario, Canada. HYSPLIT back trajectories suggest relatively rapid air mass transport to the site from the southwest. Following this event, a high-pressure system moved into the area, resulting in local stagnation. Afternoon concentrations of pollutants including ground-level ozone (60–90 ppb), SO_2 (40–70 ppb), and fine particulate matter (18–40 μg/m^3) were highly

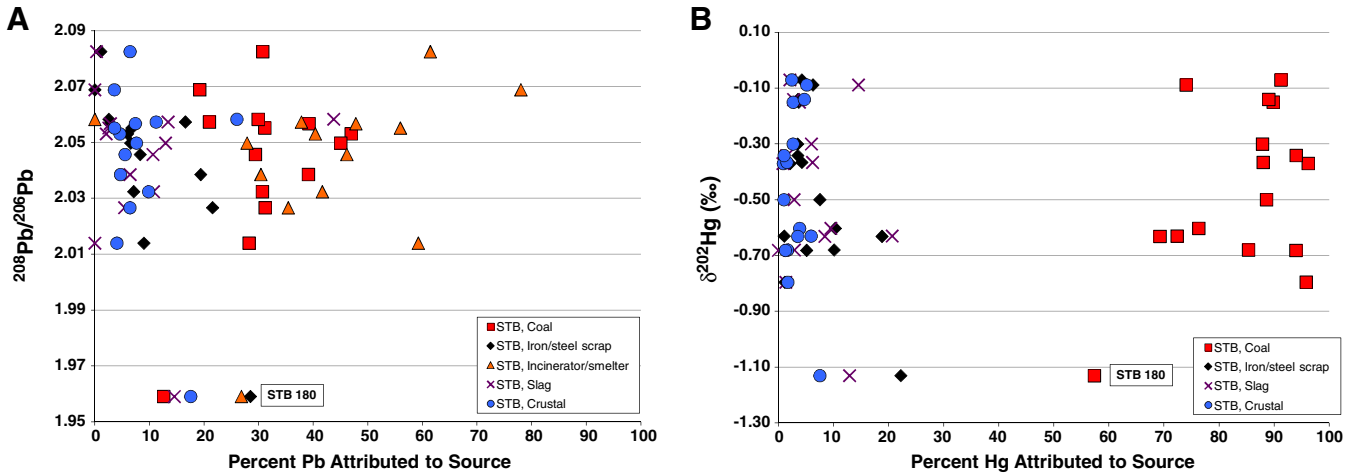

Fig. 5. Percentage of attributable metal deposition associated with sources based on PMF versus isotope ratios for Steubenville, Ohio precipitation samples. Each precipitation sample is represented by one isotope ratio (y-axis) and four or five source contributions (x-axis). Case study sample STB 180 is labeled (see Section 3.4). A). Percentages of attributable Pb deposition previously associated with each source factor by PMF (White, 2009) versus measured $^{208}Pb/^{206}Pb$ ratio. B). Percentages of attributable Hg deposition previously associated with each source factor by PMF (White, 2009) versus measured $\delta^{202}Hg$ value.

elevated for several days (U.S. EPA, AirData). In the late afternoon on August 1, 2003, a low-pressure system moved over Lake Michigan from the west, resulting in precipitation in the early morning on August 2, 2003 (4:00–6:00 UTC; sample FRT 24). As described below, it is likely that stagnation prior to this event resulted in the enhanced deposition of locally emitted pollutants at the Detroit site (sample FRT 24).

Lead isotope ratios in these Detroit samples were similar to those of samples collected in Grand Rapids, Michigan (Fig. 3). According to previous PMF estimates, Pb collected in sample FRT 23 was primarily associated with emissions from iron and steel production whereas Pb in sample FRT 24 was associated with emissions from both coal combustion and iron and steel production (UMAQL, 2009). Although sample FRT 23 exhibited slightly lower Pb isotope ratios than the other Detroit samples ($^{207}Pb/^{206}Pb = 0.8266$, $^{208}Pb/^{206}Pb = 2.0344$; Table 1), these ratios were not as low as those observed in some of the Steubenville samples or MVT Pb ores (Fig. 2). It is likely that increased recycling of metals from multiple sources makes it more difficult to identify Pb deposition resulting from iron and steel production using Pb isotope ratios.

Mercury isotope ratios measured in the Detroit precipitation samples were highly variable (Fig. 4). As shown in Fig. 6A, according to PMF estimates, in addition to coal combustion, Hg collected in sample FRT 23 was more heavily impacted by emissions from iron and steel production, likely from facilities located to the southwest of the site. This sample displayed a more negative $\delta^{202}Hg$ value ($-0.50 \pm 0.10‰$, 2SD) than the other Detroit samples. These data support the hypothesis that Hg emissions from metal processing facilities display negative $\delta^{202}Hg$ values.

The variability in $\Delta^{199}Hg$ values between the Detroit samples is even more striking (Fig. 6B). Sample FRT 24 displayed an extreme negative $\Delta^{199}Hg$ value ($-0.87 \pm 0.15‰$, 2 SD). Most analyzed rainfall samples have slightly positive $\Delta^{199}Hg$ values (Chen et al., 2012; Demers et al., 2013; Donovan et al., 2013; Gratz et al., 2010; Sherman et al., 2012) and no previous studies have measured similarly negative $\Delta^{199}Hg$ values in rainfall. As described above, rainfall during this event occurred after a period of several days of local stagnation characterized by elevated ground-level ozone, SO_2, and fine particulate matter concentrations. It is likely that these pollutants were emitted by local sources and trapped in the area by the persistent high-pressure system and light surface winds. It is possible either that locally emitted Hg displayed extreme negative $\Delta^{199}Hg$ values or that negative MIF occurred in the atmosphere during this event. Negative $\Delta^{199}Hg$ values have been observed in Arctic snow (Sherman et al., 2010) and in vegetation (Blum et al., 2012, 2014; Carignan et al., 2009; Das et al., 2012; Demers et al., 2013; Estrade et al., 2010; Tsui et al., 2012) likely due to heterogeneous photochemical reduction of Hg from snow crystals and photochemical

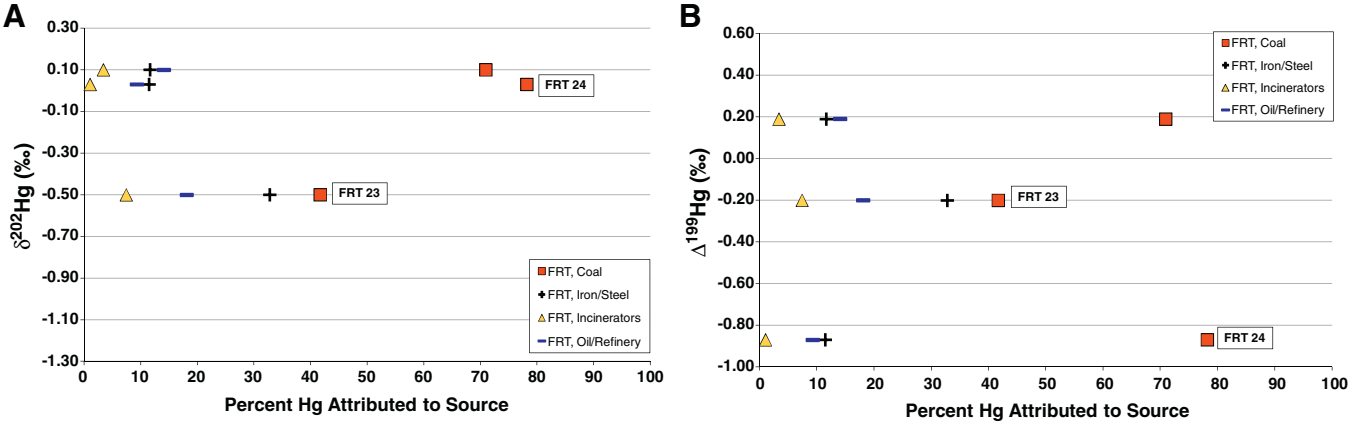

Fig. 6. Percentage of attributable Hg deposition associated with sources based on PMF versus Hg isotope ratios for Detroit, Michigan precipitation samples. Each precipitation sample is represented by one isotope ratio (y-axis) and four source contributions (x-axis). Case study samples FRT 23 and FRT 24 are labeled (see Section 3.4). A). Percentages of attributable Hg deposition previously associated with each source factor by PMF (UMAQL, 2009) versus measured $\delta^{202}Hg$ value. B). Percentages of attributable Hg deposition previously associated with each source factor by PMF (UMAQL, 2009) versus measured $\Delta^{199}Hg$ value.

reduction of thiol-bound Hg, respectively (Sherman et al., 2010; Zheng and Hintelmann, 2010). It is unlikely that these summer, low-elevation air masses (max elevation of 24-hour HYSPLIT back trajectories = 250 m) contained significant snow crystals. Additionally, highly elevated Δ^{200}Hg values, which have been suggested to indicate heterogeneous upper atmospheric processes (Chen et al., 2012), were not observed in these samples (see Appendices B and C). However, we cannot rule out the possibility that the locally stagnant conditions and elevated sulfur concentrations caused distinct atmospheric conditions resulting in the observed negative MIF. Whether the negative MIF in this sample was due to deposition of Hg emitted by an isotopically distinct Hg source or the occurrence of negative MIF in the atmosphere, these unique conditions were not discernible using trace metal concentrations and PMF receptor modeling alone.

4. Conclusions

This study represents the first combined measurement of Pb, Sr, and Hg isotope ratios in precipitation and was conducted both to explore the isotopic variability of precipitation in the Great Lakes region as well as the potential usefulness of multiple metal isotopes for identification of pollution sources. These data will improve isotopic characterization of atmospheric end-members for ecosystem isotope studies. We also observed isotopic differences between precipitation collection sites that were attributable to local and regional differences in anthropogenic source emissions such as coal combustion and MVT Pb ore processing.

In several cases, the isotopic results support previous source apportionment results based on trace element concentrations and PMF receptor modeling. For example, Pb isotope ratios suggest that a significant proportion of the Pb deposition in the Great Lakes region results from coal combustion. Observed differences in Hg and Sr isotope ratios between sites in Michigan and Ohio suggest that coal combustion is a primary source of these metals and largely controls the measured isotope ratios. In addition, Pb and Hg isotope ratios indicate that industrial sites such as Steubenville, Ohio are variably influenced by other industrial sources such as MVT Pb ore processing.

These results corroborate previous PMF receptor modeling and may be used in future modeling efforts to constrain a model's numerical solution and reduce associated uncertainties. We have demonstrated that metal isotope ratios can provide independent corroboration of these estimates and add to the "weight of evidence" needed to identify and link pollution sources with metal deposition. However, these isotopic data often do not provide a simple tracer with which to definitively identify and distinguish between source emissions. Future source attribution using multiple metal isotope ratios will require improved characterization of the isotopic composition of both raw materials and point source emissions. In addition, a more complete understanding of Hg fractionation both within industrial facilities and in the atmosphere is needed. While more research is necessary to further develop these isotopic methods for source attribution, our results suggest that the use of multiple metal isotope ratios as an additional tool for pollution source attribution holds great promise.

Acknowledgments

This work was supported in part by the University of Michigan Water Center of the Graham Sustainability Institute, which receives funds from the Fred A. and Barbara M. Erb Family Foundation and the University of Michigan. The EPA through its Office of Research and Development partially funded and participated in this research through cooperative agreement R-82971601 and contract EPD05005 with the University of Michigan. The views expressed in this manuscript are those of the authors and do not necessarily reflect the views or policies of the EPA. It has been subjected to Agency review and approved for publication. Mention of trade names or commercial products does not constitute an endorsement or recommendation for use. The authors are grateful to Jamie Gleason, Marcus Johnson, and Ted Huston for analytical assistance as well as Jim Barres, Frank Marsik, Emily White, Ali Kamal, Naima Hall, and Bian Liu for their dedicated efforts in data collection and interpretation. We also thank four anonymous reviewers for comments that improved this manuscript. Finally, this research would not have been possible without the oversight, vision, and commitment of the late Jerry Keeler.

Appendix A. Supplementary data

Supplementary data to this article can be found online at http://dx.doi.org/10.1016/j.scitotenv.2014.09.034.

References

Bailey SW, Hornbeck JW, Driscoll CT, Gaudette HE. Calcium inputs and transport in a base-poor forest ecosystem as interpreted by Sr isotopes. Water Resour Res 1996; 32:707–19.

Baustian KJ, Cziczo DJ, Wise ME, Pratt KA, Kulkarni G, Hallar AG, et al. Importance of aerosol composition, mixing state, and morphology for heterogeneous ice nucleation: a combined field and laboratory approach. J Geophys Res 2012;117:D06217. http://dx.doi.org/10.1029/2011JD016784.

Bergquist BA, Blum JD. Mass-dependent and mass-independent fractionation of Hg isotopes by photo-reduction in aquatic systems. Science 2007;318:417–20.

Biswas A, Blum JD, Bergquist BA, Keeler GJ, Zhouqing X. Natural mercury isotope variation in coal deposits and organic soils. Environ Sci Technol 2008;42:8303–9.

Blum JD, Bergquist BA. Reporting the variations in the natural isotopic composition of mercury. Anal Bioanal Chem 2007;388:353–9.

Blum JD, Erel Y. Rb–Sr isotope systematics of a granitic soil chronosequence: the importance of biotite weathering. Geochim Cosmochim Acta 1997;61:3193–204.

Blum JD, Erel Y. Radiogenic isotopes in weathering and hydrology. In: Holland HD, Turekian KK, editors. Surface and ground water, weathering and soils, 5. Oxford: Elsevier-Pergamon; 2003. p. 365–92.

Blum JD, Klaue A, Nezat CA, Driscoll CT, Johnson CE, Siccama TG, et al. Mycorrhizal weathering of apatite as an important calcium source in base-poor forest ecosystems. Nature 2002;427:729–31.

Blum JD, Johnson MW, Gleason JD, Demers JD, Landis MS, Krupa S. Mercury concentration and isotopic composition of epiphytic tree lichens in the Athabasca oil sands region. In: Percy KE, editor. Developments in environmental science: Alberta oil sands. Energy, Industry, and the EnvironmentAmsterdam, The Netherlands: Elsevier Ltd.; 2012. p. 373–90.

Blum JD, Sherman LS, Johnson MW. Mercury isotopes in earth and environmental sciences. Annu Rev Earth Planet Sci 2014;42:249–69. http://dx.doi.org/10.1146/annurev-earth-050212-124107.

Bollhöfer A, Rosman KJR. Isotopic source signatures for atmospheric lead: the Northern Hemisphere. Geochim Cosmochim Acta 2001;65:1727–40.

Brockman CS. Physiographic regions of Ohio. State of Ohio, Department of Natural Resources, Division of Geological Survey; 1998 [Available at http://www.google.com/url?sa=t&rct=j&q=&esrc=s&source=web&cd=1&ved=0CCMQFjAA&url=http%3A%2F%2Fwww.epa.state.oh.us%2Fportals%2F27%2FSIP%2FNonattain%2FF2-physiographic_regions_of_Ohio.pdf&ei=Ol4GVPvyI7K_sQTrtoDgBA&usg=AFQjCNEZyjai2r3WZY2ikGaGuXE48MTzyw&sig2=LJvry8tQ1ltsMJ4l7CeMOg&bvm=bv.74115972,d.cWc. Accessed March 2014].

Brown TD, Smith DN, Hargis RAJ, O'Dowd WJ. Mercury measurement and its control: what we know, have learned, and need to further investigate. J Air Waste Manage Assoc 1999;49:1–97.

Buchachenko AL. Magnetic isotope effect: nuclear spin control of chemical reactions. J Phys Chem 2001;105:9995–10011.

Bullen TD, Krabbenhoft DP, Kendall C. Kinetic and mineralogic controls on the evolution of groundwater chemistry and $^{87}Sr/^{86}Sr$ in a sandy silicate aquifer, northern Wisconsin, USA. Geochim Cosmochim Acta 1996;60:1807–21.

Burke WH, Denison RE, Hetherington EA, Koepnick RB, Nelson HF, Otto JB. Variation of seawater $^{87}Sr/^{86}Sr$ throughout Phanerozoic time. Geology 1982;10:516–9.

Burke J, Hoyer M, Keeler G, Scherbatskoy T. Wet deposition of mercury and ambient mercury concentrations at a site in the Lake Champlain basin. Water Air Soil Pollut 1995; 80:353–62.

Carignan J, Estrade N, Sonke JE, Donard OFX. Odd isotope deficits in atmospheric Hg measured in lichens. Environ Sci Technol 2009;43:5660–4. http://dx.doi.org/10.1021/es900578v.

Chen J, Hintelmann H, Feng X, Dimock B. Unusual fractionation of both odd and even mercury isotopes in precipitation from Peterborough, ON, Canada. Geochim Cosmochim Acta 2012;90:33–46.

Chow TJ, Earl JL. Lead isotopes in North American coals. Science 1972;176:510–1.

Clack H. Estimates of increased black carbon emissions from electrostatic precipitators during powdered activated carbon injection for mercury emissions control. Environ Sci Technol 2012;46:7327–33.

Clarkson TW, Vyas JB, Ballatori N. Mechanisms of mercury disposition in the body. Am J Ind Med 2007;50:757–64.

Cohen M, Artz R, Draxler R, Miller P, Poissant L, Niemi D, et al. Modeling the atmospheric transport and deposition of mercury to the Great Lakes. Environ Res 2004;95:247–65.

Cohen MD, Artz RS, Draxler RR. NOAA report to congress: mercury contamination in the Great Lakes. Available at http://www.google.com/url?sa=t&rct=j&q=&esrc=

s&source=web&cd=2&ved=0CCoQFjAB&url=http%3A%2F%2Fwww.arl.noaa.gov%2Fdocuments%2Freports%2FNOAA_GL_Hg_briefing.pdf&ei=_mEGVPnUDPK_sQSr3oKwAQ&usg=AFQjCNGFu1R7kbxjtTAxcv3raZBQpY6d-g&sig2=1YF11CbdvCZcElGFkH0W5w&bvm=bv.74115972,d.cWc, 2007. [Accessed March 2014].
Das R, Bizimis M, Wilson AM. Tracing mercury seawater vs. atmospheric inputs in a pristine SE USA salt marsh system: mercury isotope evidence. Chem Geol 2012;336:50–61.
Demers JD, Blum JD, Zak DR. Mercury isotopes in a forested ecosystem: implications for air-surface exchange dynamics and the global mercury cycle. Glob Biogeochem Cycles 2013;27:1–17. http://dx.doi.org/10.1002/gbc.20021.
DePaolo DJ, Ingram BL. High-resolution stratigraphy with strontium isotopes. Science 1985;227:938–41.
DesJardins MJ, Telmer K, Beauchamp S. Apportioning atmospheric pollution to Canadian and American sources in Kejimkujik National Park, Nova Scotia, using Pb isotopes in precipitation. Atmos Environ 2004;38:6875–81.
Díaz-Somoano M, Kylander ME, López-Antón MA, Suárez-Ruiz I, Martínez-Tarazona MR, Ferrat M, et al. Stable lead isotope compositions in selected coals from around the world and implications for present day aerosol source tracing. Environ Sci Technol 2009;43:1078–85.
Dockery DW, Pope CAI, Xu X, Spengler JD, Ware JH, Fay ME, et al. An association between air pollution and mortality in six U.S. cities. N Engl J Med 1993;329:1753–9.
Doe BR, Delevaux MH. Source of lead in southeast Missouri galena ores. Econ Geol 1972;67:409–25.
Donovan PM, Blum JD, Yee D, Gehrke GE, Singer MB. An isotopic record of mercury in San Francisco Bay sediment. Chem Geol 2013;349–350:87–98.
Draxler RR and Rolph GD. National Oceanic and Atmospheric Science Administration, Air Resources Laboratory, 2010. Available at http://ready.arl.noaa.gov/HYSPLIT.php. Accessed March 2014.
Dreimanis A, Goldthwait RP. Wisconsin glaciation in the Huron, Erie, and Ontario lobes. In: Black RF, Goldthwait RP, Willman HB, editors. The Wisconinan stage. Memoir, 136. Boulder, Colorado: Geological Society of America; 1973.
Dvonch JT, Graney JR, Keeler GJ, Stevens RK. Use of elemental tracers to source apportion mercury in south Florida precipitation. Environ Sci Technol 1999;33:4522–7.
Dvonch JT, Keeler GJ, Marsik FJ. The influence of meteorological conditions on the wet deposition of mercury in southern Florida. J Appl Meteorol 2005;44:1421–35.
Erel Y, Veron A, Halicz L. Tracing the transport of anthropogenic lead in the atmosphere and in soils using isotopic ratios. Geochim Cosmochim Acta 1997;61:4495–505.
Estrade N, Carignan J, Sonke JE, Donard OFX. Mercury isotope fractionation during liquid–vapor evaporation experiments. Geochim Cosmochim Acta 2009;73:2693–711. http://dx.doi.org/10.1016/j.gca.2009.01.024.
Estrade N, Carignan J, Donard OFX. Isotope tracing of atmospheric mercury sources in an urban area of northeastern France. Environ Sci Technol 2010;44:6062–7. http://dx.doi.org/10.1021/es100674a.
Evers DC, Savoy LJ, DeSorbo CR, Yates DE, Hanson W, Taylor KM, et al. Adverse effects from environmental mercury loads on breeding common loons. Ecotoxicology 2008;17:69–81.
Fitzgerald WF, Mason RP, Vandal GM. Atmospheric cycling and air–water exchange of mercury over mid-continental lacustrine regions. Water Air Soil Pollut 1991;56:745–67.
Flegal AR, Nriagu JO, Niemeyer S, Coale KH. Isotopic tracers of lead contamination in the Great Lakes. Nature 1989;339:455–8.
Flores RM, Hanley JH. Anastomosed and associated coal-bearing fluvial deposits: Upper Tongue River Member, Palaeocene Fort Union Formation, northern Powder River Basin, Wyoming, U.S.A. In: Rahmani RA, Flores RM, editors. Sedimentology of coal and coal-bearing sequences. The International Association of Sedimentologists; 1984.
Geagea ML, Stille P, Millet M, Perrone T. REE characteristics and Pb, Sr and Nd isotopic compositions of steel plant emissions. Sci Total Environ 2007;373:404–19.
Glass GE, Sorensen JA. Six-year trend (1990–1995) of wet mercury deposition in the upper Midwest, U.S.A. Environ Sci Technol 1999;33:3303–12.
Goldhaber MB, Church SE, Doe BR, Aleinikoff JN, Brannon JC, Podosek FA, et al. Lead and sulfur isotope investigation of Paleozoic sedimentary rocks from the southern midcontinent of the United States: implications for paleohydrology and ore genesis of the southeast Missouri lead belts. Econ Geol 1995;90:1875–910.
Graney JR, Landis MS. Coupling meteorology, metal concentrations, and Pb isotopes for source attribution in archived precipitation samples. Sci Total Environ 2013;448:141–50.
Graney JR, Halliday AN, Keeler GJ, Nriagu JO, Robbins JA, Norton SA. Isotopic record of lead pollution in lake sediments from the northeastern United States. Geochim Cosmochim Acta 1995;59:1715–28.
Gratz LE, Keeler GJ. Sources of mercury in precipitation to Underhill, VT. Atmos Environ 2011;45:5440–9.
Gratz LE, Keeler GJ, Miller EK. Long-term relationships between mercury wet deposition and meteorology. Atmos Environ 2009;43:6218–29.
Gratz LE, Keeler GJ, Blum JD, Sherman LS. Isotopic composition and fractionation of mercury in Great Lakes precipitation and ambient air. Environ Sci Technol 2010;44:7764–70. http://dx.doi.org/10.1021/es100383w.
Gratz LE, Keeler GJ, Marsik FJ, Barres JA, Dvonch JT. Atmospheric transport of speciated mercury across southern Lake Michigan: influence from emission sources in the Chicago/Gary urban area. Sci Total Environ 2013a;448:84–95. http://dx.doi.org/10.1016/j.scitotenv.2012.08.076.
Gratz LE, Keeler GJ, Morishita M, Barres JA, Dvonch JT. Assessing the emission sources of atmospheric mercury in wet deposition across Illinois. Sci Total Environ 2013b;448:120–31. http://dx.doi.org/10.1016/j.scitotenv.2012.11.011.
Gray JE, Pribil MJ, Van Metre PC, Borrok DM, Thapalia A. Identification of contamination in a lake sediment core using Hg and Pb isotopic compositions, Lake Ballinger, Washington, USA. Appl Geochem 2013;29:1–12.
Grousset FE, Biscaye PE. Tracing dust sources and transport patterns using Sr, Nd and Pb isotopes. Chem Geol 2005;222:149–67.
Haack UK, Gutsche FH, Plessow K, Heinrichs H. On the isotopic composition of Pb in cloud waters in central Germany: a source discrimination study. Water Air Soil Pollut 2002;139:261–88.
Hall BD, Manolopoulos H, Hurley JP, Schauer JJ, St. Louis VL, Kenski D, et al. Methyl and total mercury in precipitation in the Great Lakes region. Atmos Environ 2005;39:7557–69.
Heckel PH. Glacial-eustatic base-level — climatic model for late middle to late Pennsylvanian coal-bed formation in the Appalachian Basin. J Sediment Res 1995;B65:348–56.
Hedman KM, Curry BB, Johnson TM, Fullagar PD, Emerson TE. Variation in strontium isotope ratios of archaeological fauna in the Midwestern United States: a preliminary study. J Archaeol Sci 2009;36:64–73.
Herrick GT, Friedland AJ. Patterns of trace metal concentration and acidity in montane forest soils of the northeastern United States. Water Air Soil Pollut 1990;53:151–7.
Heyl AV, Landis GP, Zartman RE. Isotopic evidence for the origin of Mississippi Valley-type mineral deposits: a review. Econ Geol 1974;69:992–1006.
Hodell DA, Mead GA, Mueller PA. Variation in the strontium isotopic composition of seawater (8 Ma to present): implications for chemical weathering rates and dissolved fluxes to the oceans. Chem Geol 1990;80:291–307.
Hoyer M, Burke J, Keeler G. Atmospheric sources, transport and deposition of mercury in Michigan: two years of event precipitation. Water Air Soil Pollut 1995;80:199–208.
Hurst RW, Davis TE. Strotium isotopes as tracers of airborne fly ash from coal-fired power plants. Environ Geol 1981;3:363–7.
Hurst RW, Davis TE, Elseewi AA. Strontium isotopes as tracers of coal combustion residue in the environment. Eng Geol 1991;30:59–77.
Hurst RW, Davis TE, Elseewi AA, Page AL. Strontium and lead isotopes as monitors of fossil fuel dispersion. In: Keefer RF, Sajwan KS, editors. Trace elements in coal and coal combustion residues. United States: Lewis Publishers; 1993.
Kaste JM, Friedland AJ, Stürup S. Using stable and radioactive isotopes to trace atmospherically deposited Pb in montane forest soils. Environ Sci Technol 2003;37:3560–7.
Keeler GJ, Dvonch JT. Atmospheric mercury: a decade of observations in the Great Lakes. In: Pirrone N, Mahaffey KR, editors. Dynamics of mercury pollution on regional and global scales: atmospheric processes and human exposures around the world. US, New York, New York: Springer; 2005. p. 611–36.
Keeler GJ, Gratz LE, Al-Wali K. Long-term atmospheric mercury wet deposition at Underhill, Vermont. Ecotoxicology 2005;14:71–83.
Keeler GJ, Landis MS, Norris GA, Christianson EM, Dvonch JT. Sources of mercury wet deposition in eastern Ohio, USA. Environ Sci Technol 2006;40:5874–81.
Komárek M, Ettler V, Chrastný V, Mihaljevič M. Lead isotopes in environmental sciences: a review. Environ Int 2008;34:562–77.
Kritee K, Blum JD, Johnson MW, Bergquist BA, Barkay T. Mercury stable isotope fractionation during reduction of Hg(II) to Hg(0) by mercury resistant microorganisms. Environ Sci Technol 2007;41:1889–95.
Kritee K, Barkay T, Blum JD. Mass dependent stable isotope fractionation of mercury during *mer* mediated microbial degradation of monomethylmercury. Geochim Cosmochim Acta 2009;73:1285–96.
Landis MS, Keeler GJ. Critical evaluation of a modified automatic wet-only precipitation collector for mercury and trace element determinations. Environ Sci Technol 1997;31:2610–5.
Landis MS, Keeler GJ. Atmospheric mercury deposition to Lake Michigan during the Lake Michigan Mass Balance Study. Environ Sci Technol 2002;36:4518–24.
Landis MS, Vette AF, Keeler GJ. Atmospheric mercury in the Lake Michigan Basin: influence of the Chicago/Gary urban area. Environ Sci Technol 2002;36:4508–17.
Laraque D, Trasande L. Lead poisoning: successes and 21st century challenges. Pediatr Rev 2005;26:435–43.
Lefticariu L, Blum JD, Gleason JD. Mercury isotopic evidence for multiple mercury sources in coal from the Illinois Basin. Environ Sci Technol 2011;45:1724–9.
Lin C-J, Pehkonen SO. The chemistry of atmospheric mercury: a review. Atmos Environ 1999;33:2067–79.
Liu B, Keeler GJ, Dvonch JT, Barres JA, Lynam MM, Marsik FJ, et al. Temporal variability of mercury speciation in urban air. Atmos Environ 2007;41:1911–23.
Liu B, Keeler GJ, Dvonch JT, Barres JA, Lynam MM, Marsik FJ, et al. Urban–rural differences in atmospheric mercury speciation. Atmos Environ 2010;44:2013–23.
Ma J, Hintelmann H, Kirk JL, Muir DCG. Mercury concentrations and mercury isotope composition in lake sediment cores from the vicinity of a metal smelting facility in Flin Flon, Manitoba. Chem Geol 2013;336:96–102.
McArthur JM, Howarth RJ, Bailey TR. Strontium isotope stratigraphy: LOWESS Version 3: best fit to the marine Sr–isotope curve for 0–509 Ma and accompanying look-up table for deriving numerical age. J Geol 2001;109:155–70.
McArthur JM, Rio D, Massari F, Castradori D, Bailey TR, Thirlwall M, et al. A revised Pliocene record for marine-$^{87}Sr/^{86}Sr$ used to date an interglacial event recorded in the Cockburn Island Formation, Antarctic Peninsula. Palaeogeogr Palaeoclimatol Palaeoecol 2006;242:126–36.
Miller EK, Blum JD, Friedland AJ. Determination of soil exchangeable-cation loss and weathering rates using Sr isotopes. Nature 1993;362:438–41.
National Pollutant Release Inventory. Available at http://www.ec.gc.ca/inrp-npri/, 2008. [Accessed January 2010].
National Weather Service, Colorado State University. NWS DIFAX weather map archive. Available at http://archive.atmos.colostate.edu/. [Accessed May 2014].
Nriagu JO, Pacyna JM. Quantitative assessment of worldwide contamination of air, water and soils by trace metals. Nature 1998;333.
Paatero P. Least squares formulation of robust non-negative factor analysis. Chemometr Intell Lab Syst 1997;37:23–35.
Pacyna EG, Pacyna JM, Steenhuisen F, Wilson S. Global anthropogenic mercury emission inventory for 2000. Atmos Environ 2006;40:4048–63.

Parker JL, Bloom NS. Preservation and storage techniques for low-level aqueous mercury speciation. Sci Total Environ 2005;337:253–63.
Pirrone N, Cinnirella S, Feng X, Finkelman RB, Friedli HR, Leaner J, et al. Global mercury emissions to the atmosphere from anthropogenic and natural sources. Atmos Chem Phys 2010;10:5951–64.
Rabinowitz MB. Lead isotopes in soils near five historic American lead smelters and refineries. Sci Total Environ 2005;346:138–48.
Rabinowitz MB, Wetherill GW. Identifying sources of lead contamination by stable isotope techniques. Environ Sci Technol 1972;6:705–9.
Risch MR, Gay DA, Fowler KK, Keeler GJ, Backus SM, Blanchard P, et al. Spatial patterns and temporal trends in mercury concentrations, precipitation depths, and mercury wet deposition in the North American Great Lakes region, 2002–2008. Environ Pollut 2012;161:261–71.
Rodríguez-González P, Epov VN, Bridou R, Tessier E, Guyoneaud R, Monperrus M, et al. Species-specfic stable isotope fractionation of mercury during Hg(II) methylation by an anaerobic bacteria (*Desulfobulbus propionicus*) under dark conditions. Environ Sci Technol 2009;43:9183–8.
Rolison JM, Landing WM, Luke W, Cohen M, Salters VJM. Isotopic composition of species-specific atmospheric Hg in a coastal environment. Chem Geol 2013;336:37–49.
SAS Institute Inc. SAS 9.4; 2013 [Available at http://www.sas.com/en_us/software/sas9.html].
Schroeder WH, Munthe J. Atmospheric mercury — an overview. Atmos Environ 1998;32:809–22.
Shen GT, Boyle EA. Lead in corals: reconstruction of historical industrial fluxes to the surface ocean. Earth Planet Sci Lett 1987;82:289–304.
Sherman LS, Blum JD, Johnson KP, Keeler GJ, Barres JA, Douglas TA. Mass-independent fractionation of mercury isotopes in Arctic snow driven by sunlight. Nat Geosci 2010;3:173–7. http://dx.doi.org/10.1038/ngeo758.
Sherman LS, Blum JD, Keeler GJ, Demers JD, Dvonch JT. Investigation of local mercury deposition from a coal-fired power plant using mercury isotopes. Environ Sci Technol 2012;46:382–90. http://dx.doi.org/10.1021/es202793c.
Simonetti A, Gariépy C, Carignan J. Pb and Sr isotopic evidence for sources of atmospheric heavy metals and their deposition budgets in northeastern North America. Geochim Cosmochim Acta 2000a;64:3439–52.
Simonetti A, Gariépy C, Carignan J. Pb and Sr isotopic compositions of snowpack from Québec, Canada: inferences on the sources and deposition budgets of atmospheric heavy metals. Geochim Cosmochim Acta 2000b;64:5–20.
Simonetti A, Gariépy C, Carignan J, Poissant L. Isotopic evidence of trace metal sources and transport in eastern Canada as recorded from wet deposition. J Geophys Res 2000c;105:12264–78.
Sonke JE, Schafer J, Chmeleff J, Audry S, Blanc G, Dupre B. Sedimentary mercury stable isotope records of atmospheric and riverine pollution from two major European heavy metal refineries. Chem Geol 2010;279:90–100.
Spivak-Birndorf LJ, Stewart BW, Capo RC, Chapman EC, Schroeder KT, Brubaker TM. Strontium isotope study of coal utilization by-products interacting with environmental waters. J Environ Qual 2012;41:144–54.
Stancin AM, Gleason JD, Rea DK, Owen RM, Moore TCJ, Blum JD, et al. Radiogenic isotopic mapping of late Cenozoic eolian and hemipelagic sediment distribution in the east-central Pacific. Earth Planet Sci Lett 2006;248:840–50.
Straughan IR, Elseewi AA, Page AL, Kaplan IR, Hurst RW, Davis TE. Fly ash-derived strontium as an index to monitor deposition from coal-fired power plants. Science 1981;212:1267–9.
Sturges WT, Barrie LA. Lead 206/207 isotope ratios in the atmosphere of North America as tracers of US and Canadian emissions. Nature 1987;329:144–6.
Sturges WT, Barrie LA. The use of stable lead 206/207 isotope ratios and elemental composition to discriminate the origins of lead in aerosols at a rural site in eastern Canada. Atmos Environ 1989;23:1645–57.
Sturges WT, Hopper JF, Barrie LA, Schnell RC. Stable lead isotope ratios in Alaskan arctic aerosols. Atmos Environ 1993;27A:2865–71.
Sun R, Heimbürger L-E, Sonke JE, Liu G, Amouroux D, Berail S. Mercury stable isotope fractionation in six utility boilers of two large coal-fired power plants. Chem Geol 2013;336:103–11. http://dx.doi.org/10.1016/j.chemgeo.2012.10.055.
Sun R, Sonke JE, Heimbürger L-E, Belkin HE, Liu G, Shome D, et al. Mercury stable isotope signatures of world coal deposits and historical coal combustion emissions. Environ Sci Technol 2014;48:7660–8.
Swaine DJ. Trace elements in coal. London: Butterworth; 1990.
Tsui MTK, Blum JD, Kwon SY, Finlay JC, Balogh SJ, Nollet YH. Sources and transfers of methylmercury in adjacent river and forest food webs. Environ Sci Technol 2012;46:10957–64. http://dx.doi.org/10.1021/es3019836.
U.S. Energy Information Administration. Monthly utility and nonutility fuel receipts and fuel quality data, EIA-423. Available at http://www.eia.gov/electricity/data/eia423/, 2004–2005. [Accessed January 2014].
U.S. Environmental Protection Agency. National emissions inventory. Available at http://www.epa.gov/ttnchie1/net/2008inventory.html, 2005. [Accessed January 2010].
U.S. Environmental Protection Agency. $PM_{2.5}$ filterable and PM_{10} filterable emissions trends for electric generating utilities for 1970 to 2005. Process optimization guidance for reducing mercury emissions from coal combustion in power plants: a report from the coal combustion partnership area; 2008.
U.S. Environmental Protection Agency. 2008 biennial national listing of fish advisories; 2009 [EPA-823-F-09-007].
U.S. Environmental Protection Agency. AirData. Available at http://www.epa.gov/airquality/airdata/. [Accessed March 2014].
U.S. Environmental Protection Agency, Office of Research and Development. EPA positive matrix factorization (PMF) 5.0 fundamentals & user guide; 2014 [Report No. EPA-600.R-14.108].
University of Michigan Air Quality Laboratory (UMAQL). Monitoring atmospheric mercury species in Michigan: final report, submitted to Great Lakes Protection Fund and the Great Lakes Commission. 2009. [Available at https://www.yumpu.com/en/document/view/6428905/monitoring-atmospheric-mercury-species-in-michigan-great-lakes-. Accessed December 2013].
University of Michigan, Department of Atmospheric, Oceanic, and Space Sciences. Shared air: trajectories to air quality monitoring sites. Available at http://www.sharedair.org, 2012. [Accessed March 2014].
University of Wyoming, College of Engineering. Upper air soundings. Available at http://weather.uwyo.edu/upperair/sounding.html. [Accessed March 2014].
Vedantham R, Landis MS, Olson D, Pancras P. Source identification of $PM_{2.5}$ in Steubenville, Ohio using a hybrid method for highly time-resolved data. Environ Sci Technol 2014;48:1718–26.
Veron AJ, Church TM, Flegal AR, Patterson CC, Erel Y. Response of lead cycling in the surface Sargasso Sea to changes in tropospheric input. J Geophys Res 1993;98:18269–76.
Weis D, Kieffer B, Maerschalk C, Barling J, de Jong J, Williams GA, et al. High-precision isotopic characterization of USGS reference materials by TIMS and MC-ICP-MS. Geochem Geophys Geosyst 2006;7:30.
White EM. Source attribution, physicochemical properties and spatial distribution of wet deposited mercury to the Ohio River Valley [Ph.D. Thesis] Ann Arbor: Department of Atmospheric, Oceanic and Space Sciences; 2009. p. 145 [Available at http://deepblue.lib.umich.edu/bitstream/handle/2027.42/63813/emwhite_1.pdf?sequence=1].
White EM, Keeler GJ, Landis MS. Spatial variability of mercury wet deposition in eastern Ohio: summertime meteorological case study analysis of local source influences. Environ Sci Technol 2009;43:4946–53.
White EM, Landis MS, Keeler GJ, Barres JA. Investigation of mercury wet deposition physicochemistry in the Ohio River Valley through automated sequential sampling. Sci Total Environ 2013;448:107–19.
Yin R, Feng X, Meng B. Stable mercury isotope variation in rice plants (*Oryza sativa* L.) from the Wanshan mercury mining district, SW China. Environ Sci Technol 2013;47:2238–45.
Yin R, Feng X, Chen J. Mercury stable isotope compositions in coals from major coal producing fields in China and their geochemical and environmental implications. Environ Sci Technol 2014;48:5565–74.
Zheng W, Hintelmann H. Isotope fractionation of mercury during its photochemical reduction by low-molecular-weight organic compounds. J Phys Chem A 2010;114:4246–53. http://dx.doi.org/10.1021/jp9111348.
Zheng W, Foucher D, Hintelmann H. Mercury isotope fractionation during volatilization of Hg(0) from solution into the gas phase. J Anal At Spectrom 2007;22:1097–104.